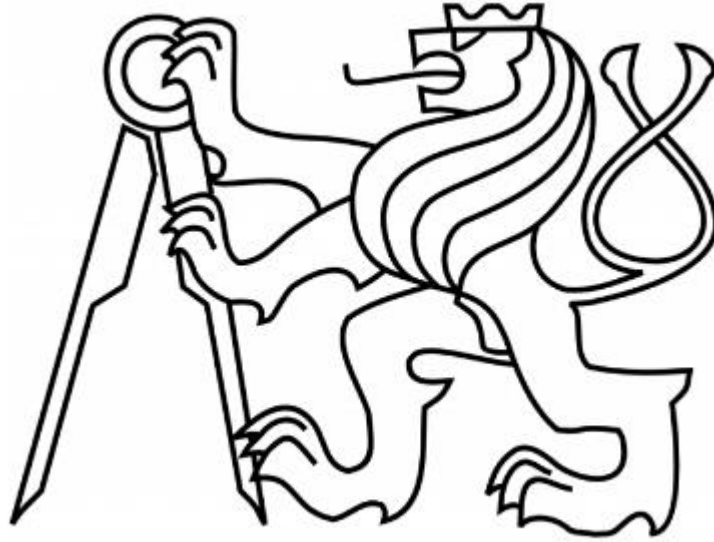


Czech Technical University in Prague

Faculty of mechanical engineering



Diploma thesis

Design of the Brake Pad Impedance Test Rig

Prague, 2016

Vojtěch Schovánek

TASK OF DIPLOMA THESIS

For: Vojtěch Schovánek

Program: Master degree program

Field of study: Vehicles

Title (English): Design of the Brake Pad Impedance Test Rig

Title (Czech): Návrh zkušební stolice pro měření impedance brzdového obložení

Instructions for work:

1. State of the art
2. Propose concepts of solution
3. Design selected concept
4. FEA of selected concept

Declaration of originality

I hereby declare that this thesis and the work reported herein was composed by and originated entirely from me. Information derived from the published and unpublished work of others has been acknowledged in the text and references are given in the list of sources.

Prague, 2016

.....

Acknowledgement

I would like to express my sincere to all my advisers, Dipl.-Ing Sergio Carvajal, Ing. Ondřej Jakubský Ph.D., Ing. Zdeněk Podzemný, Ing Petr Sedláček Ph.D., and to my supervisor Ing. Michal Vašíček Ph.D. for their valuable guidance, support and training given throughout this work. I also want thank to my family for their help and encouragement during the whole study.

Annotation

Diploma thesis is focused on development of brake pad mechanical impedance test rig. This is mainly feasibility study and different approaches comparison. Demands analysis is complemented by brief state of the art, followed by concepts description and final approach decision. Thesis is finished by FEM simulation of contact pressure and modal analysis of the whole rig.

Anotace

Diplomová práce je zaměřena na vývoj stolice pro měření mechanické impedance brzdového obložení. Jedná se především o studii proveditelnosti a porovnání odlišných přístupů. Rozbor požadavků na stolicí je doplněn o stručnou rešerši, následuje popis konceptů a rozhodnutí o konečném přístupu. Práce je zakončena MKP simulací kontaktního tlaku a modální analýzou celé stolice.

Keywords

Brake pad test rig, mechanical impedance, brake pressure distribution, modal analysis

Klíčová slova

Testovací stolice brzdového obložení, mechanická impedance, rozložení brzdového tlaku, modální analýza

Table of content

1 Introduction	8
2 Test rig demands	9
2.1 Realistic brake pad support and clamping	10
2.2 Excitation demands.....	12
2.3 Measurement and processing of the measured quantities.....	13
2.4 General demands on the device	14
3 State of the art - Used methods	15
3.1 Mechanical impedance	15
3.2 Methods of brake pads simulations.....	15
3.2.1 Complex eigenvalue analysis.....	16
3.2.2 Dynamic transient analysis	17
3.3 Acceleration sensors.....	18
3.4 Force sensors	20
4 Development of the concepts.....	21
4.1 Preloading possibilities	22
4.1.1 Hydraulic preloading	22
4.1.2 Electromagnetic preloading.....	23
4.1.3 Mechanical preloading	25
4.2 Excitation possibilities	26
4.3 Concept 1	28
4.4 Concept 2	29
4.5 Concept 3	30
4.6 Concept 4	32
4.7 Concept 5	33

4.8 Concepts evaluation	35
5 Determination of selected concept.....	36
5.1 Brake pad test models	37
5.1.1 Smaller brake pad.....	37
5.1.2 Bigger brake pad.....	39
5.2 Geometry development.....	42
5.2.1 Concept 2.....	43
5.2.2 Concept 3.....	45
5.2.3 Concept 5.....	46
5.4 Final concept geometry.....	49
6 FEM analysis.....	51
6.1 FE model	52
6.1.1 Mesh properties	52
6.1.2 Constraints.....	53
6.1.3 Preloading.....	55
6.2 Results.....	57
6.2.1 Pressure distribution	57
6.2.2 Modal shapes, sensitivity with smaller pad	59
6.2.3 Modal shapes, sensitivity with bigger pad.....	64
6.3 Results validity.....	69
6.2.3 Dependence of eigenfrequency on friction coefficient.....	69
6.3.2 Bending of the rig.....	72
7 Conclusions.....	73
References.....	74

1 Introduction

Brake pad noise appeared at the same time as brakes themselves. It does not affect performance, but driving comfort decreases, which is important especially for high-class vehicles. Even though there are many various approaches to avoid brake noise, this problem has not been resolved yet. Noise, which is caused by relative motion between brake pad and disc, is affected by lot of variable quantities. Brake squeal usually appears in the range from 1 kHz to 16 kHz and as well as other vibrations, it depends on mechanical behaviour of oscillating features. [1]

This thesis is focused on developing method of lining material mechanical parameters description. In classical modal analysis, brake pad is free and its modal shapes are significantly different to behaviour in real conditions. Main goal is to develop test rig, which is able to make modal analysis of brake pad in real clamping conditions. Kinematics and stiffness of the rig determines pad deformations similar to brake assembly. Friction motion is avoided and excitation is done by vibration exciter, but the brake pad should be preloaded as much as similar to the brake calliper. This means, that experimental modal analysis is made with the whole test rig, and not just a free brake pad. Modal behaviour of this assembly must be sensitive to lining material elastic properties for possible identification of lining material Young modulus and shear modulus. From measured data in forms of accelerations and forces, mechanical impedance can be computed.

Purpose of this test rig is based on problematic behaviour of friction material. Due to the complicated technology of brake pads manufacturing, elastic properties of this material are scattered widely. This complicates evaluation of squeal tendency. For description of brake pad noise behaviour, prestressed modal analysis seems to be good working tool.

2 Test rig demands

Requirements for classical modal analysis, such as the possibility of introducing excitation and sensors location, are complemented by the requirement of pretension. Practically, it is necessary to press the brake pad between at least two other parts. The first represents a brake disc and the second one a callipers with hydraulic pistons and guide pins. Additional parts are usually needed for applying a pre-load.

2.1 Realistic brake pad support and clamping

One of the biggest problems of this rig is clamping the pad. Boundary conditions in the rig must be as similar as possible to the boundary conditions in real calipers. This means that forces should be introduced as shown in figure 1.

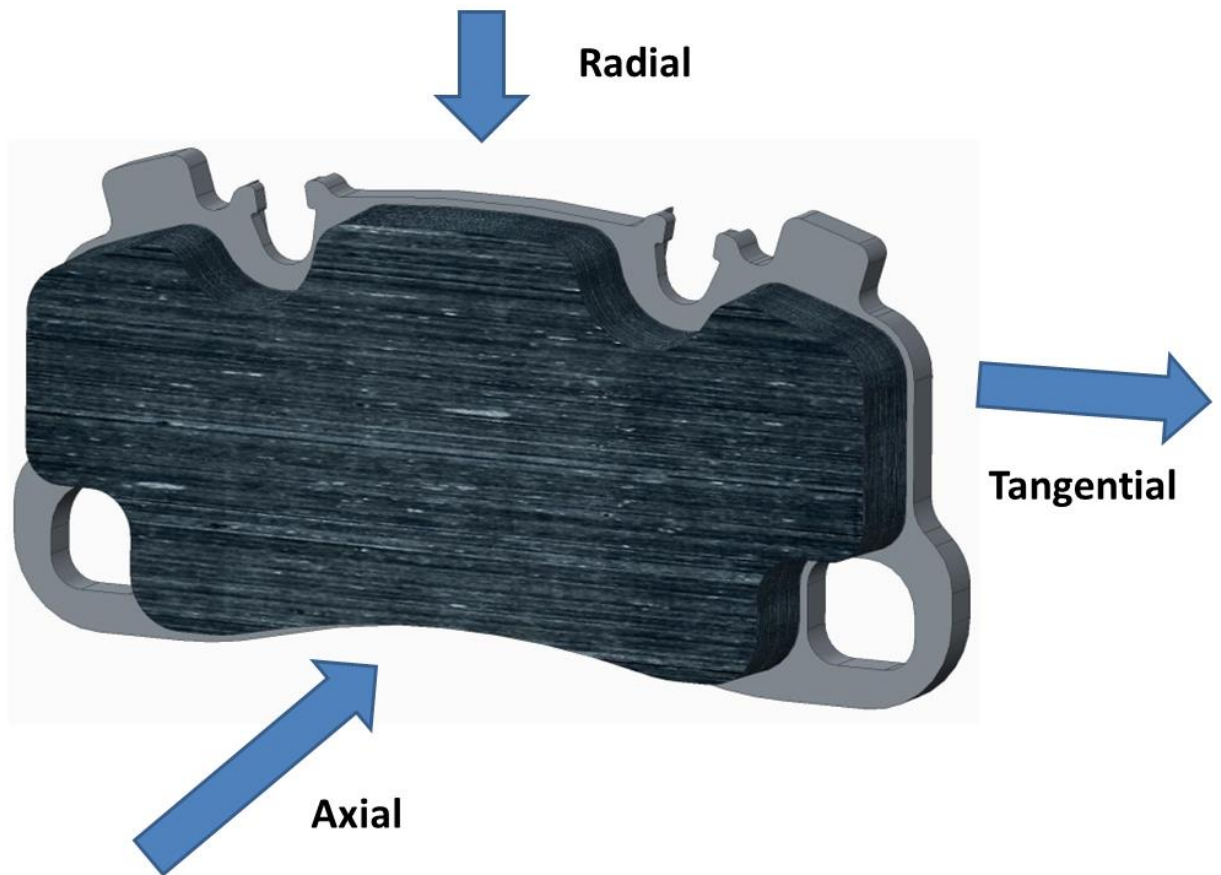


Figure 1 Force components

These forces can be decomposed by cylindrical coordinate system like in real conditions into following components:

Radial force pushes the pad to the centre of disc rotation. In real caliper, this force is introduced by sheet metal spring and the main purpose is to define brake pad position on pins. The position is important for introduction of braking forces in right placements and for interception of reactions in required directions. This is the reason, why this force must be applied first. Radial component of total force is negligible in comparison with the other two force components.

Axial force corresponds to the piston force caused by hydraulic pressure. This is the action force and depends on the intensity of braking. It pushes the pad against the

disc. Magnitude of the force corresponds to hydraulic pressure 2 MPa (20 Bar) and is the biggest of all the forces. Options of introduction of this force component are wide, but limited by its magnitude. Possibilities will be discussed later.

Tangential force is a result of axial force and relative motion between brake disc and brake pad in real conditions. This force component acts against the direction of rotation and is desired result of braking. Tangential force is a function of axial force and always takes smaller values than axial force- depends on the friction coefficient and usually equals 40 % of axial force.

The actual size of these forces depends on the specific type of brakes and brake pads, as well as forces location, because calipers differ in numbers and positions of hydraulic pistons and guide pins. Practically, for the universal test condition there must be variable adjustments to the force size and the area of effect. The effect area depends primarily on the pistons location. This limits the versatility of the test rig.

2.2 Excitation demands

Excitation should be done by the shaker, actuating right on the friction material of the brake pad in frequency range of 2Hz – 7kHz. If possible, excitation frequency should reach 10kHz. There is demand for excitation of assembly in all Cartesian directions individually, specifically in radial, axial and tangential direction. This is usually achieved by suitably dimensioned rod between test rig and shaker. This rod transfers longitudinal load much more than transversal load. This idea is shown in figures of chapter 4.2 Excitation possibilities.

Practically this means that for excitation in axial direction it is necessary to have a drilled hole in the test rig body for introduction of connection rod between shaker and friction material. This is disadvantageous for contact pressure distribution, because of the location of the hole, the rig is not able to transfer axial and tangential force. Moreover, surrounding area is also affected. Requirement of universality makes this question more difficult, because it is nearly impossible to place this hole without mentioned effect for all sizes pads. For this reason the possibility of axial excitation through the test rig body is allowed.

Radial and axial excitation is less complicated, because friction material is better obtainable. There is a demand for good working constraint between connecting rod and friction material.

2.3 Measurement and processing of the measured quantities

All the forces introduced have to be measured. Measurement of the clamping forces must be static for exact preloading and dynamic for measuring changes during the modal analysis. Excitation force has to be measured as well. Acquisition of the excitation force value is requested through the complete range of frequency, this means from 2 Hz to 10 kHz. Acquisition of the frequency response is expected in the form of accelerations on the brake lining and back plate in the complete frequency range. Measured signals should be represented in the time and frequency domain. The complete process is shown in figure 2.

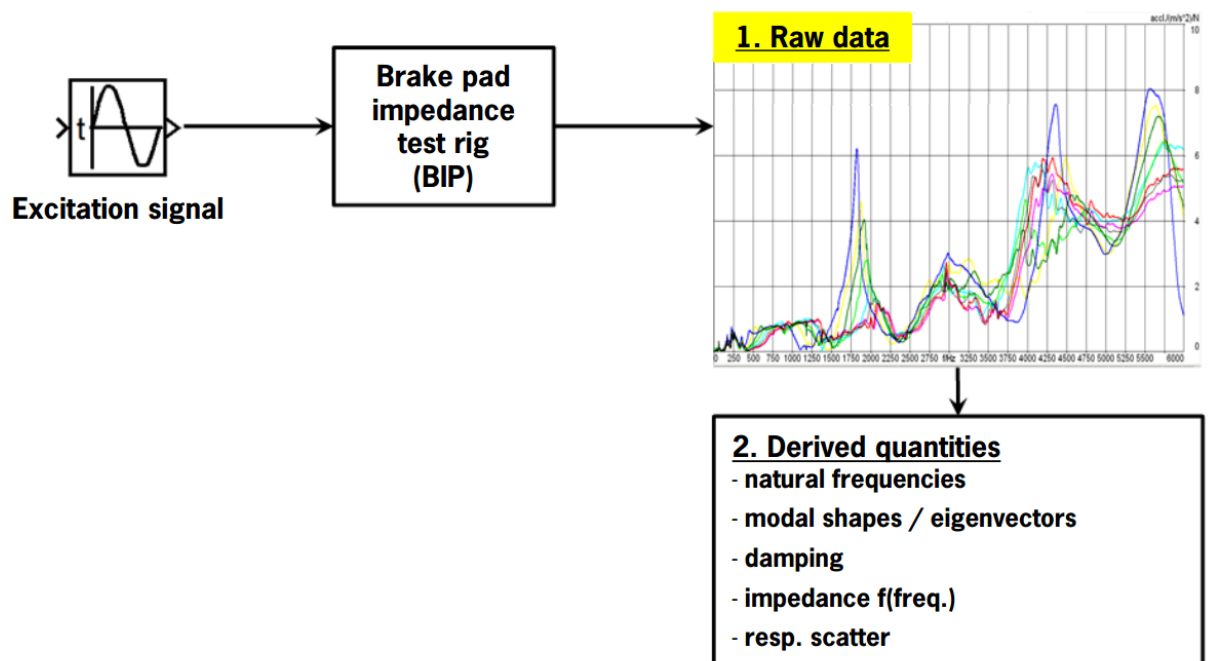


Figure 2 Schematic description of the process

Graphic representation of the modal shapes of the friction lining and determination of the mechanical impedance at various measuring points in the time and frequency domain is requested. These data will be used for mechanical impedance calculation.

2.4 General demands on the device

Very important demand is to avoid the influence of the rig itself (inconvenient dynamic behaviour) on the measured quantities. This means that the test rig must be as stiff as possible, but also it must allow friction part deformation to develop modal shapes caused by this compliant material. If the rig fixes brake pad too strictly, the pad cannot deform and even though the friction material properties change, results of modal analysis would be very similar. Changes of results would be hidden in the scatter and measuring would be useless.

Practical requests of the test rig are represented by simple operability and long life. Assembly of the rig should be mobile, so the total weight should be less than 50 kilograms. Practically, this means one man mobility and operability. The whole assembly must be corrosion resistant and made of steel. Therefore assembly needs some surface finish for the rust protection.

3 State of the art - Used methods

Development of brake pad impedance test rig is a very complex work. There have been many approaches done to test the lining material. Most of tests work with the whole brake assembly, it means caliper with pads, brake rotor and accessories. This project is unique by development of caliper substitution to better understanding of lining material dynamic behaviour. [2][3]

3.1 Mechanical impedance

Output of this rig should be mechanical impedance of the lining material. Dynamic behaviour of parts is now an important factor in design. Mechanical impedance defines the relationships between forces and motion at various points, both respect to amplitude and phase. Mechanical impedance is reciprocal quantity to mobility, so the mass at resonance has minimal impedance. [4]

Mechanical impedance is set by equation:

$$Z(\omega) = \frac{F(\omega)}{v(\omega)}$$

Where $F(\omega)$ stands for force and $v(\omega)$ stands for velocity. It means that for evaluation of brake pad impedance is necessary to know forces acting to the pad and its velocity. These quantities must be available as functions of excitation frequency. In result, rig must be able to measure preloading forces and accelerations dynamic. [5]

3.2 Methods of brake pads simulations

There are many models for analysing disc brake behaviour. Most of methods for squeal prediction are based on simulation of brake pad and brake disc assembly. Brake disc has a crucial influence on assembly behaviour and its consideration is necessary for brake squeal prediction. [1]

Finite element methods for squeal occurrence prediction can be divided to two main categories: complex eigenvalue analysis and Dynamic transient analysis. Both methods work with simulation of rotational motion and both have their pros and cons. They are briefly described below.

3.2.1 Complex eigenvalue analysis

The main idea of the complex eigenvalue method includes symmetry arguments of the stiffness matrix and the formulation of a friction coupling. This method is supposed to be more efficient than dynamic transient analysis and providing more insight to the friction-induced dynamic instability of the disc brake system. [6]

Squeal propensity is quantified by the dynamic instability of a specific system mode. Numerous examples can be found, especially for low frequency squeal. In this frequency region noise insulators are normally not much effective. Anyway, the effectiveness of countermeasures changes case by case such that a good solution for a certain brake system may have only little effect on another one. Design needs to be developed from the information provided by both the analytical and experimental efforts until the complete brake squeal mechanism is understood. [6][7]

Complex eigenvalues with positive real parts are identified as unstable modes, which always appear in complex conjugate pairs. When the damping matrix is negligible, both roots of a complex pair have virtually the same imaginary values and the real values have opposite signs. Eigenvectors are also the same except for an opposite sign of the phase angles. Detail formulation of the friction stiffness matrix for friction induced vibration can be found in the literature. Procedure of this method is shown in figure 3. [7]

In order to apply this theory to a physical system, such as a disc brake, the following additional simplifications are needed:

1. Linear elastic and homogeneous material properties.
2. The friction coefficient μ between the rotor and the lining surfaces is supposed to be constant.
3. The speed of the traveling vibration wave is supposed to be much higher than the speed of the rotor surface.
4. Absolutely planar contact between the rotor and the lining surfaces. [8]

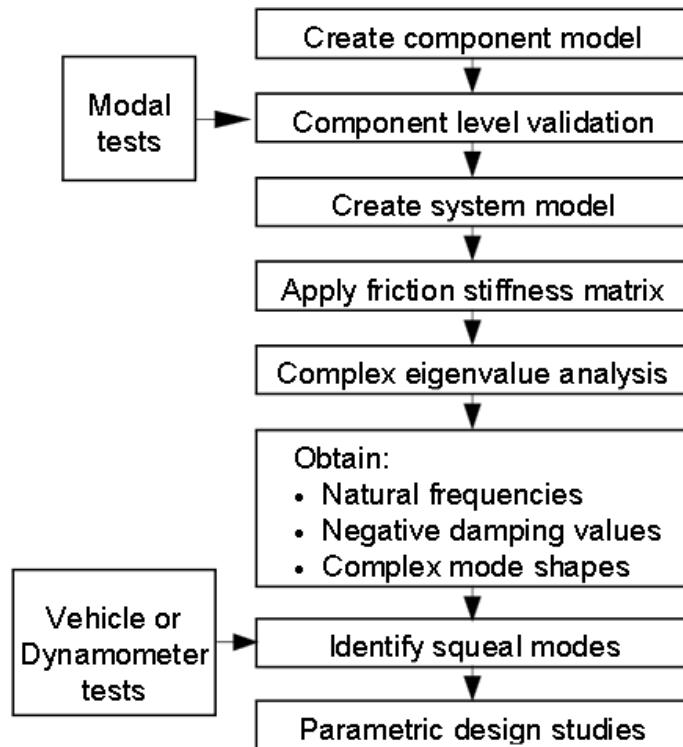


Figure 3 Complex eigenvalue analysis procedure [7]

3.2.2 Dynamic transient analysis

For the transient analysis, the time history of the brake-line pressure and rotational speed are used for describing operating conditions of the disc brake model. This is shown in figure 4. Firstly, a brake pressure is applied gradually until it reaches t_1 , and then it stays constant. The disc starts to rotate at t_1 and the speed linearly increases up to t_2 . Then the rotational speed becomes constant too. For investigation, a friction coefficient is usually constant value, obtained from squeal experiments. [8]

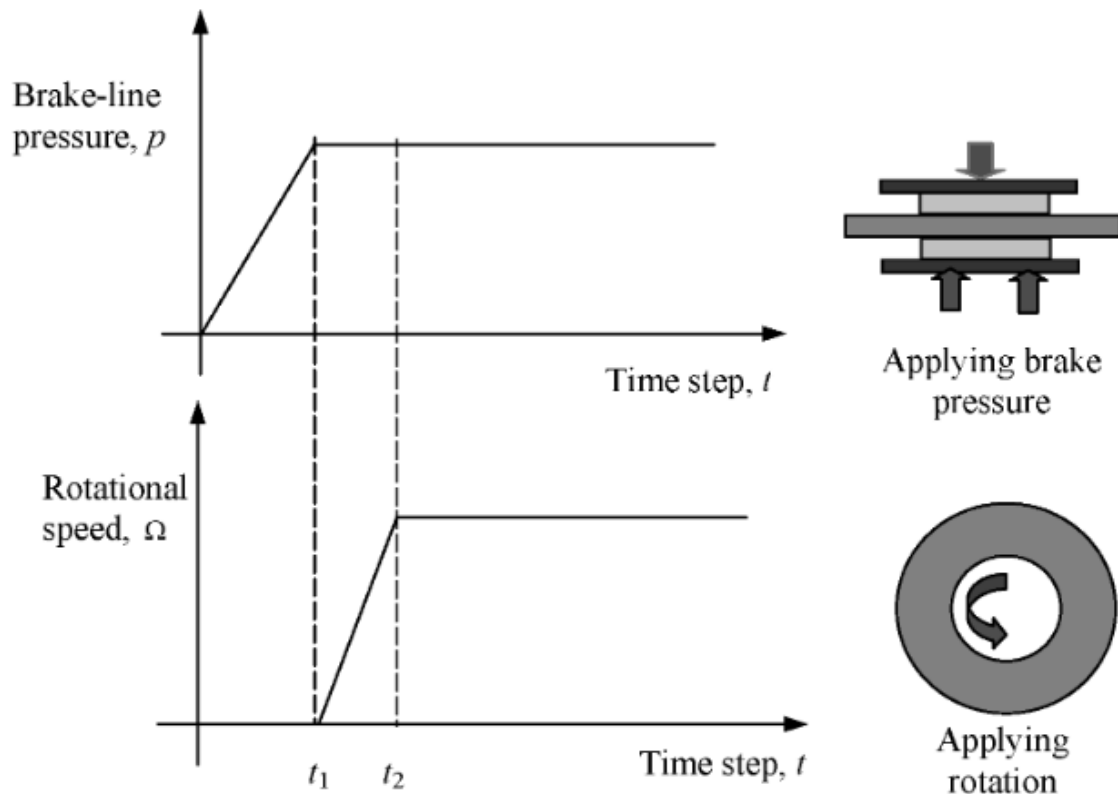


Figure 4 Schematic diagram of transient analysis procedure [8]

Currently the complex eigenvalue method is preferred to dynamic transient analysis. It is widely used in predicting the squeal propensity of the brake system including contact and damping, since the transient dynamic analysis is computationally expensive. It is important to note that both analysis approaches are performed in the absence of material and friction damping and thermal effect. [8]

3.3 Acceleration sensors

Accelerometer is a tool, which measures vibration or acceleration of structure. Typical important parameters are bandwidth and sensitivity. Requested bandwidth is set by excitation demands, it means from 2 Hz to 10 kHz. Generally, the more sensitive accelerometer is better. This means that for a given change in acceleration, there will be a larger change in signal enabling more accurate measuring. This is connected to accelerometer mass. The less mass has larger amplitudes and provides more sensitivity. In figure 5, principle of piezoelectric accelerometer is shown. [12]

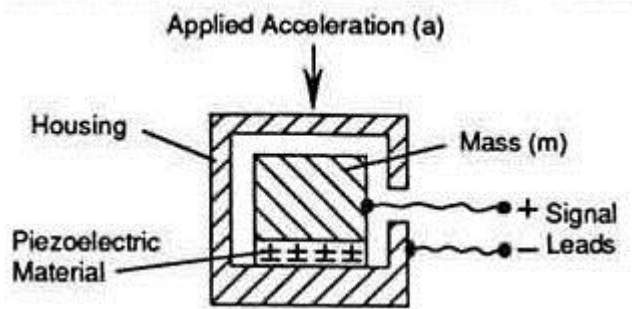


Figure 5 Piezoelectric accelerometer principle [13]

For measuring accelerations in all directions simultaneously, there must be placed for example 3 single axis accelerometers. It means that they have to be positioned separately and result is less conclusive. Placing some three axes accelerometers on interesting location at structure (with large amplitudes at important eigenfrequencies) seems to be better working option.

3.4 Force sensors

Each sensor mounted on structure means additional mass and contact. For better results, these negative effects should be decreased as much as possible.

Force is a vector, so it has always its direction. Sensors are usually able to measure force magnitude only in one direction, so it must be taken in consideration before their location and orientation. Force sensor types are strongly affected by the preloading system. Three different types of sensors were considered: tensometer, load washers (figure 6) and tension force transducers (figure 7). All mentioned sensor types are described and shown in chapter 4 with their application on concepts.



Figure 6 HBM force sensor – washer type [14]



Figure 7 Compression and tension sensor Noshok [15]

4 Development of the concepts

The originality of this project negatively affects the amount of inspirational sources. On the other hand, there are some areas with wide range of possibilities and their combination gives an opportunity to design the rig. This chapter is devoted to discussion about preliminary solutions.

Some of the demands to the test rig are contradictory. Imitation of such a complex device, like the brake is, cannot be done easily with perfect results. It was necessary to set satisfying compromise between demanded criteria. For development of the concepts, some criteria were prioritised to the others. This chapter of the project should show the possible kinematic options, even though some of them would be technologically complicated. In practise it is not possible to make simple assembly test rig with possibility of perfect clamping of various size brake pads. It is the reason why each concept emphasizes only some of desired attributes. Following discussion should eliminate unsatisfactory disadvantages and choose optimal option, eventually create appropriate compromise and set the solution by combining various concepts.

Before designing of concepts, some technical solutions had been excluded to reduce amount of possible variants. The reasons are mostly practical and total cost reducing.

4.1 Preloading possibilities

Preloading possibilities can be divided to three main approaches.

4.1.1 Hydraulic preloading

Hydraulic pre-loading would perfectly imitate real caliper conditions. It would be possible to use some serial parts, like hydraulic pistons and sealing. Hydraulic pressure could be initiated by another piston, which could be controlled by a screw. Solution with associated tangential piston is schematically shown in figure number 8.

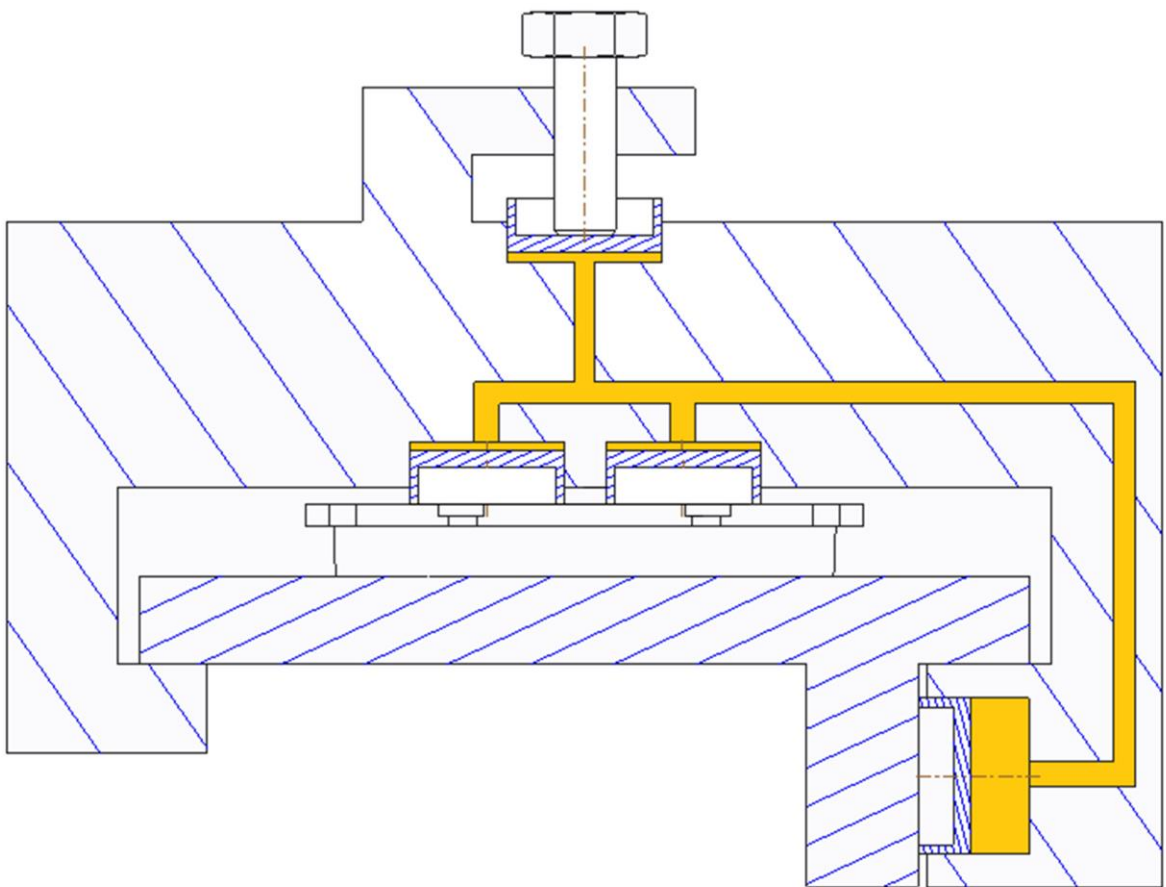


Figure 8: Scheme of hydraulic preloading

Disadvantages of hydraulic pre-stressing are noticeable. Hydraulic oil and rubber sealing are significant sources of damping, which would generate problems in describing of lining material behaviour. The next problem is the fact, that the axial and tangential forces are applied simultaneously. For exact introduction of these forces, there must be two separated hydraulic circles and the rig would be heavy with too

large influence on modal analysis results. Forces can be computed directly from the hydraulic pressure.

4.1.2 Electromagnetic preloading

Another way of pre-loading is electromagnetic. Using the solenoid actuators allows to substitute all hydraulics and to generate exact value of force on each piston. Structure of solenoid actuator is described in figure 9.

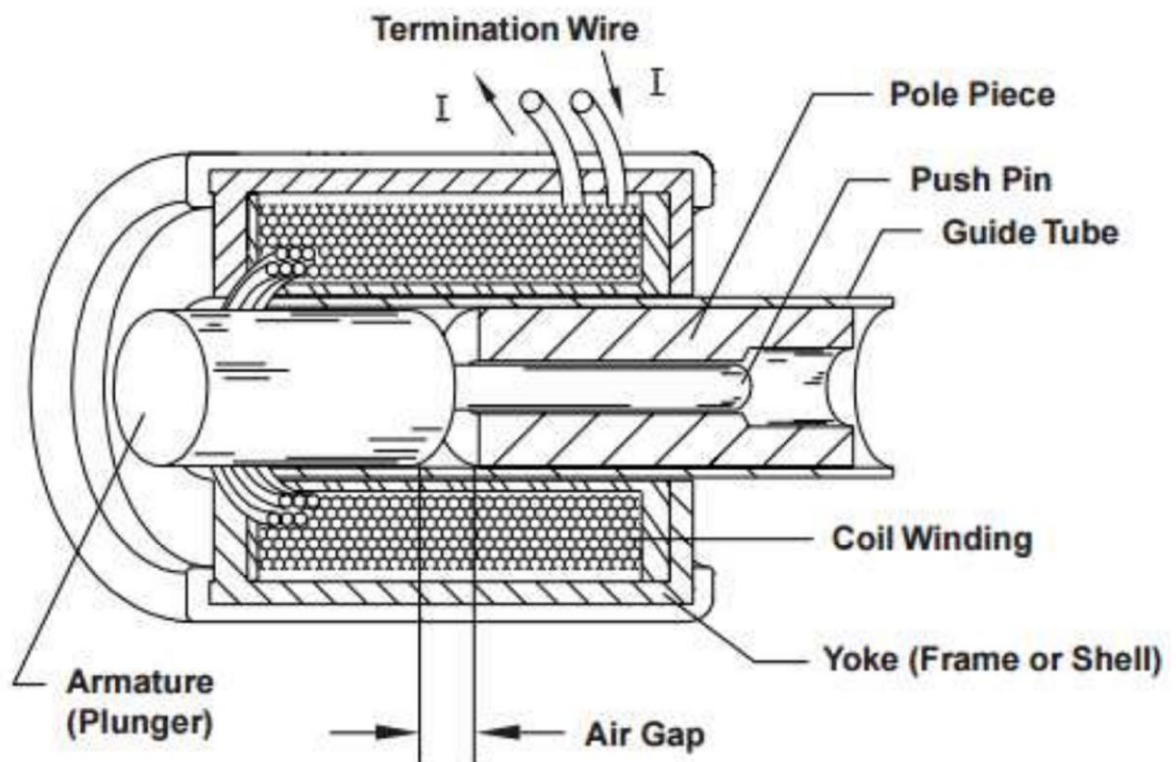


Figure 9: Solenoid actuator [16]

This type of actuator allows generating large forces on short strokes, which is desirable behaviour. Preloading, controlled by computer, can be very fast and comfortable. Version with electromagnetic preloading is shown in figure 10.

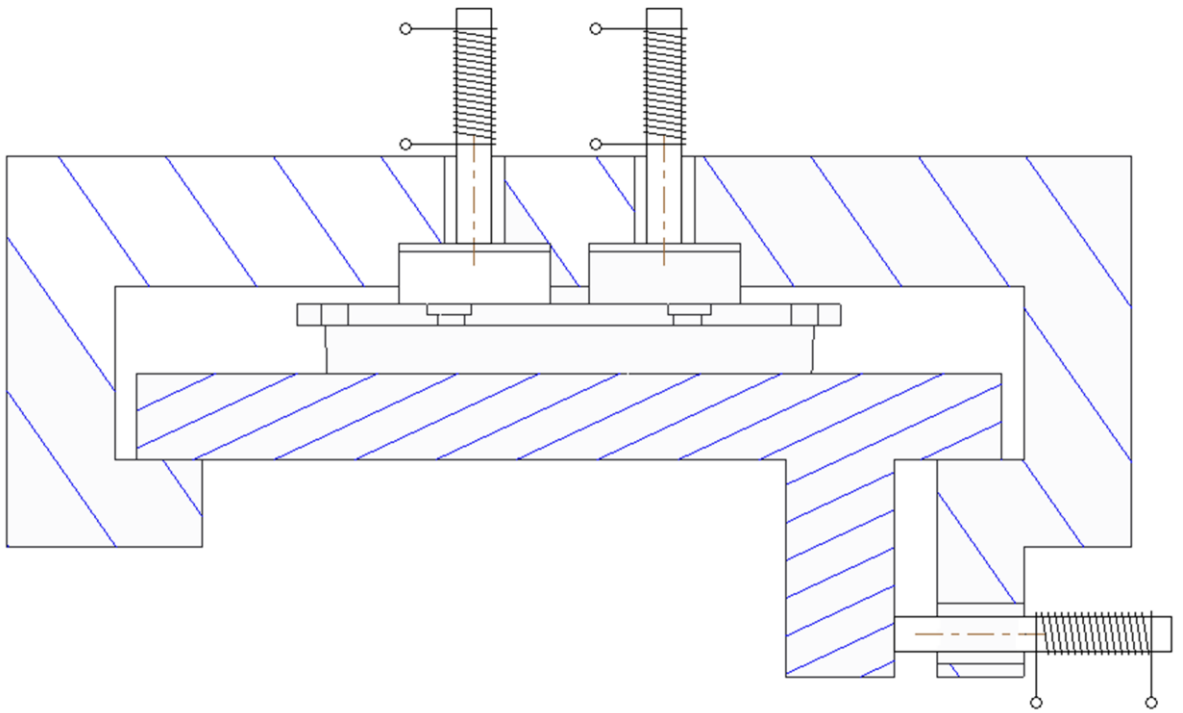


Figure 10: Scheme of electromagnetic preloading

There is a requirement of force in order of kiloNewtons. For accomplishing these magnitudes identical to brake caliper, actuators have to be large and still connected to power supply. This means possibility of forces instability, which is undesirable. There will be too much components (for example power supply wires, etc.) affecting eigenfrequencies, so the sensitivity will be decreased and the repeatability worse.

4.1.3 Mechanical preloading

The last way of introducing preloading forces is mechanical one. For linear preloading characteristics, it is favourable to use threads. Each piston is controlled by its own bolt, as shown in figure 11.

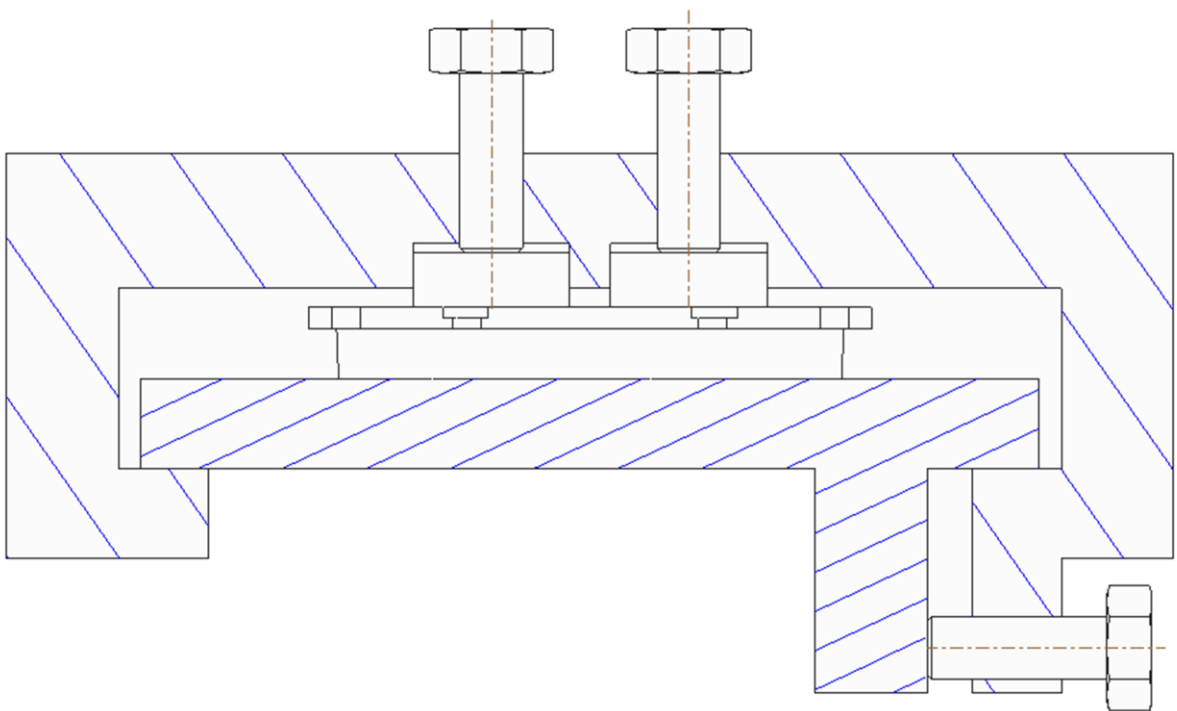


Figure 11: Scheme of mechanical preloading

Unlike the hydraulic and the electrical solution, axial force cannot be achieved on all the pistons simultaneously. This complicates pre-stressing, because when desired force magnitude is achieved on the first bolt and the pre-stressing sequence continues to the next bolt, it results in relaxing the first bolt pre-stress. In the end, it takes a long time to pre-stress multi-piston assembly and causes worse repeatability.

Mechanical preloading is the simplest possible. This is the reason, why it was chosen as the most satisfactory for the continuation of this project. This type of preloading can be realised in various ways, which are described in individual concepts

4.2 Excitation possibilities

Excitation demands are following: measured structure has to be excited by harmonic signal through frequency range 2Hz – 10kHz. In FEM analysis, total assembly could be rigidly clamped, or absolutely free. Practically, measured structure and exciter always interact with surroundings.

Free situating of tested structure is usually made by hanging on very compliant springs or laying on the foam. Both of these constraints must have defined stiffness, so the rigid body modes of modal analysis are not zero. All these eigenfrequencies should be maximally at 10 % of the lowest deformed eigenfrequency. [9]

Situating of the exciter has the same option as the structure. Three combinations of situating were discussed. Free structure and fixed exciter (figure 12) is one of the typical ideas. Clamping of the exciter has only little impact on eigenfrequencies of measured structure. [9]

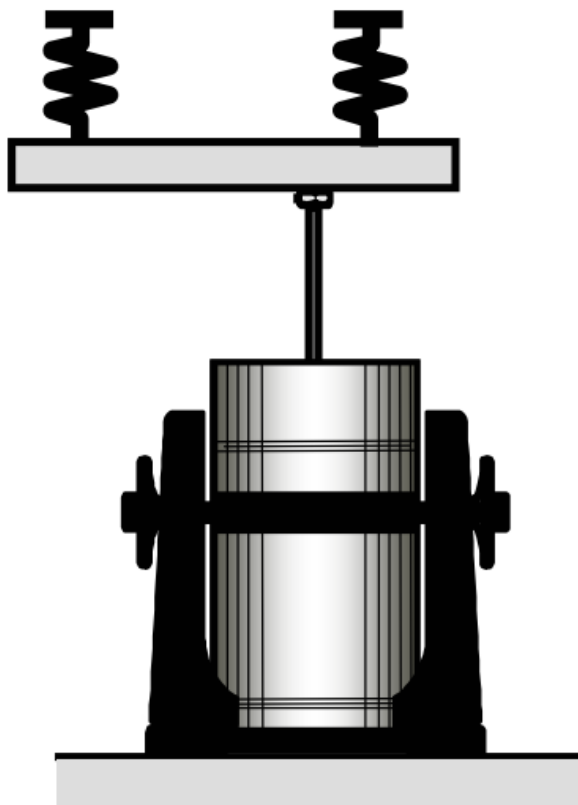


Figure 12 Free structure and fixed exciter [9]

An arrangement of fixed structure and free exciter was also discussed. It allows making structure much more stiff and moving the eigenfrequencies upwards. Either way, it means several extra conjunctions. Practically, repeatability decreases even though the structure is clamped by torque wrench, eigenfrequencies usually change by $\pm 5\%$. This arrangement is shown in figure 13. [9]

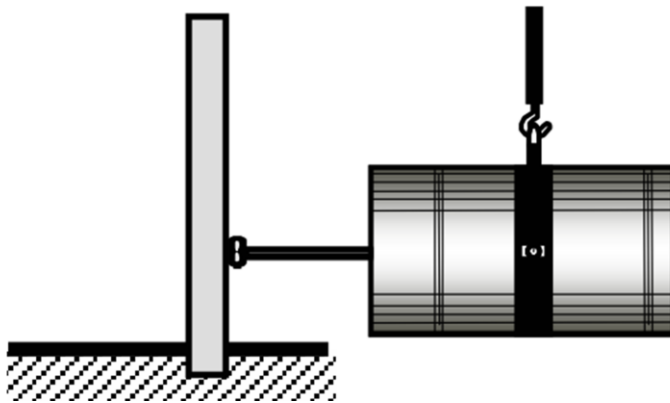


Figure 13: Free exciter and fixed structure [9]

The last usable combination is to situate exciter and structure free. Both can be laid on the foam or hanged on compliant springs. It doesn't have complicated demands and stays reliable in repeated measuring. That is the reason for choosing this solution for following work. Principle is shown in figure 14.

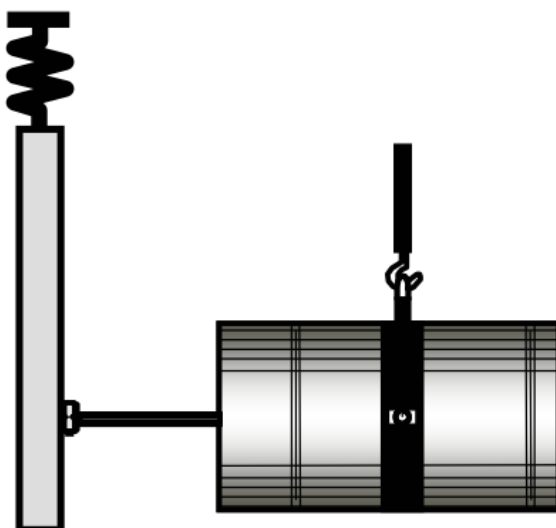


Figure 14 Free exciter and free structure [9]

4.3 Concept 1

The idea of the first concept is based on the simplest possible prestressing. All the required forces are introduced by a single screw. Preloading force of the screw is distributed to axial and tangential direction by parallelogram.

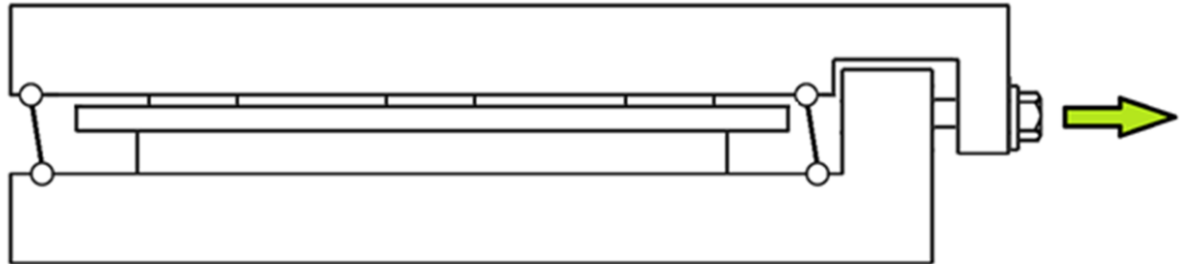


Figure 15: Concept 1 scheme, top view

These arms have joints on both ends, so they don't transfer momentum. That is suitable for placing tensometers, because the arms are not bent. For deciphering orthogonal force components, it is necessary to measure an angle of at least one arm as well.

This solution allows high repeatability, because difference of the only one prestressing force is the smallest possible. On the other hand, parallelogram generates lot of problems. Ratio between axial and tangential force is a function of the brake pad thickness. This function probably could be linearised, because deformations are small, but linearisation would be unique for each brake pad with unique thickness. There is even a possibility of slippage for too thick pads, when the angle of the arms is too large and ratio between tangential and axial force is adversely low. To avoid this fact, adjustable length of parallelogram would be a solution. This would be done with additional components, but advantage of simple loading would be lost.

Another problem could be inserting brake pad into the rig. For this reason, the arms have to be long, what makes them more compliant, or they have to be easily removable. This concept was found to be unsatisfactory.

4.4 Concept 2

Second concept also prefers simple preloading, but with nearly opposite way. The first concept has rotating parts with changeless length, this concept has shifting parts with constant angles. Forces are introduced directly through to force sensors. These transducers of tension and compression are mounted in slanted position, so the clamping force is distributed to axial and tangential components in strict ratio 5:1. This ratio is directly tangential of mounting angle, so this angle is approximately $11^{\circ} 19'$. It could be even more, but there is a hazard of exceeding the friction coefficient. This would mean the slippage of brake pad to the side. In the corners of the test rig are located 4 sensors.

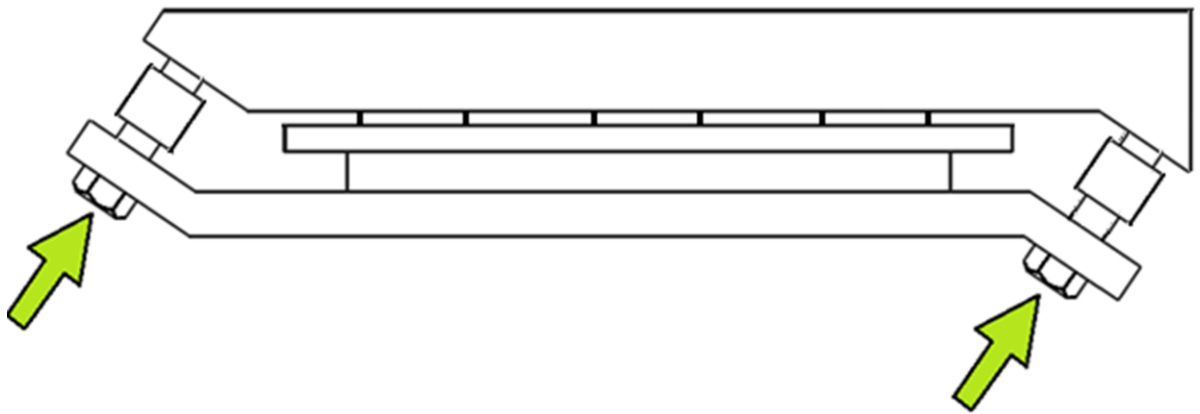


Figure 16: Concept 2 scheme, top view

The advantage of a simple clamping is also a disadvantage because it is impossible to set the forces ratio. This type of sensor also makes assembly stiffer in tangential direction, so the shear modes of modal analysis are suppressed. Sensors create additional reactions instead and disable brake pad deformations. What's more, sensors are not able to measure these forces. As a result, understanding of friction material behaviour is more complicated.

4.5 Concept 3

The third concept tries to imitate real conditions by using rotational constraint. Tangential force is really circumferential and its magnitude is a function of radius. Improvement of clamping parameters results in increasing of total mass, which is unwanted.

The first revision of this concept contains preloading by thread constraint on the main pin. It allows introduction of axial and tangential forces at the same time. This variant of test rig has only two parts with one common contact. However, this simple mechanical idea would practically generate too much problems. For modal analysis, it is necessary to lock the screw conjunction and prevent losing of preload. It means to suppress the motion between halves of the rig. When it is not moving, it doesn't allow brake pad to deform in shear modes and the pin advantage disappears.

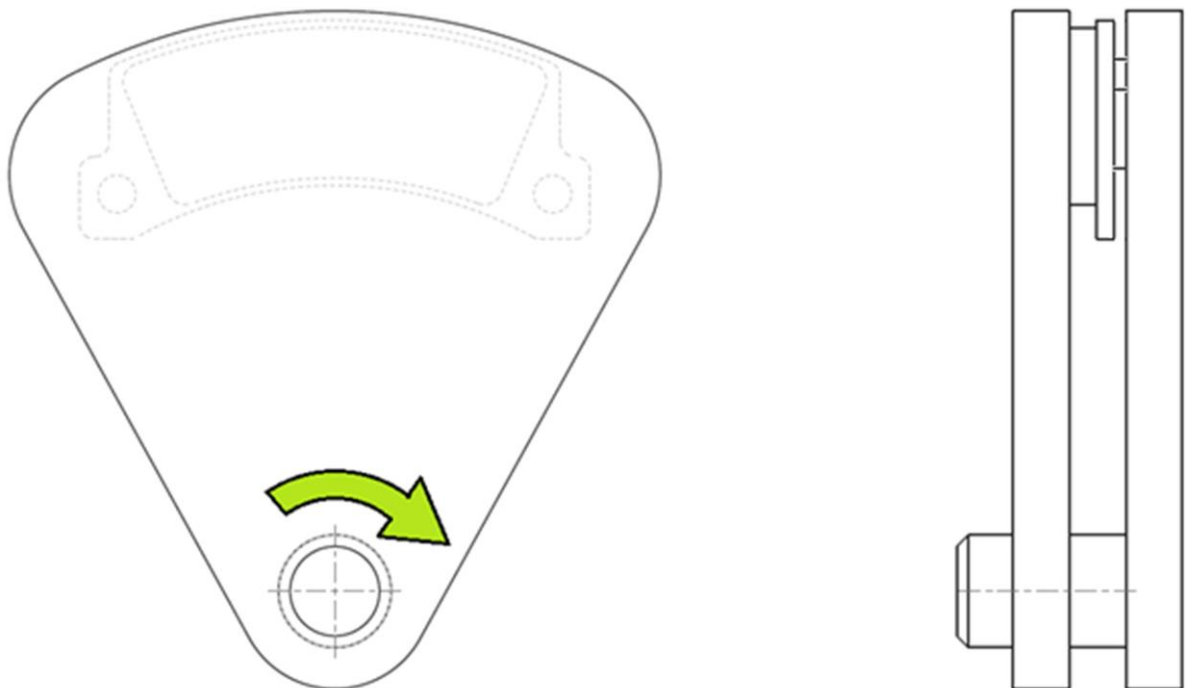


Figure 17: Concept 3 scheme, front and side view

The second revision relies on simple cylindrical pin without thread. It is missing ability of preloading and has to be accompanied by additional parts, but it satisfies modal analysis demands. Pin decreases degrees of freedom and defines the shapes of eigenfrequencies, where the rotational motion between rig halves is very common. In these shapes, brake pad is deformed in shear mode. That is very similar to real

conditions and gives this concept potential to be able to describe friction material behaviour. Preloading could be realised for example by wires with threaded ends, which are like long bolts.

Although the pin generates some desired modal shapes (for example shear mode), it also negatively influences measurement results. This extra constraint generates damping and needs to be discussed. There is a simultaneous motion in axial and tangential direction. To reduce friction in one direction as much as possible, rolling bearing is the best working approach. But for this compound motion there is a need for combination of linear and radial bearing. This means lot of rolling elements, oscillating during modal analysis. Each element has its own momentum of inertia and two contacts.

4.6 Concept 4

Concept number 4 has the most complicated system of preloading, which can be utilised for simulating conditions of brake caliper with various piston diameters. Each piston is controlled by its own bolt, between them is a compress force sensor. One screw without piston is oriented perpendicular to others for initiation of tangential force. Variability of this preloading gives a freedom in creating arbitrary contact pressure distribution with possibility of achieving the most real conditions.

This concept is complicated, because it has a lot of parts with possibility of relative motion. Especially cylindrical constraints are realised with gaps, so the exact placement is not easily repeatable. Each contact generates friction in modal analysis, which is hard to describe and makes the correlation of simulation and measurement more problematic.

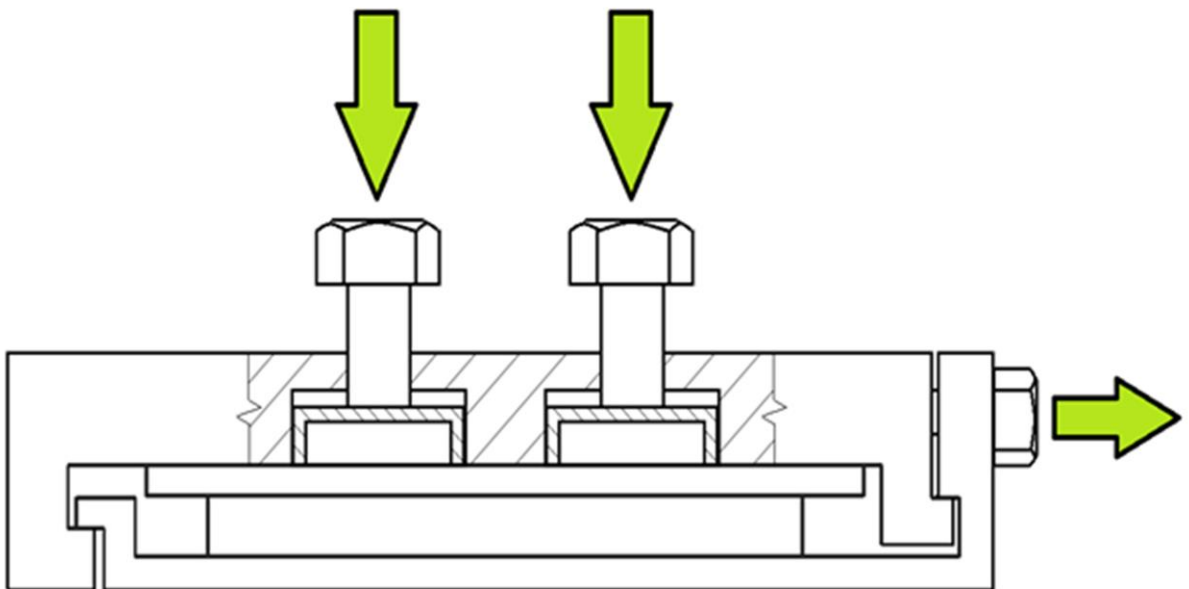


Figure 18: Concept 4 scheme, top view

4.7 Concept 5

Concept number 5 maximally eliminates influence of the rig on modal analysis results. Brake pad is clamped between very stiff halves and all constraints are compliant. They are realised by wires, which are preloaded like strings on a guitar. Wires can carry huge loads in longitudinal direction, but the load in transversal direction is several order lower. The ends of wires are like plastic joints and allow the brake pad to deform.

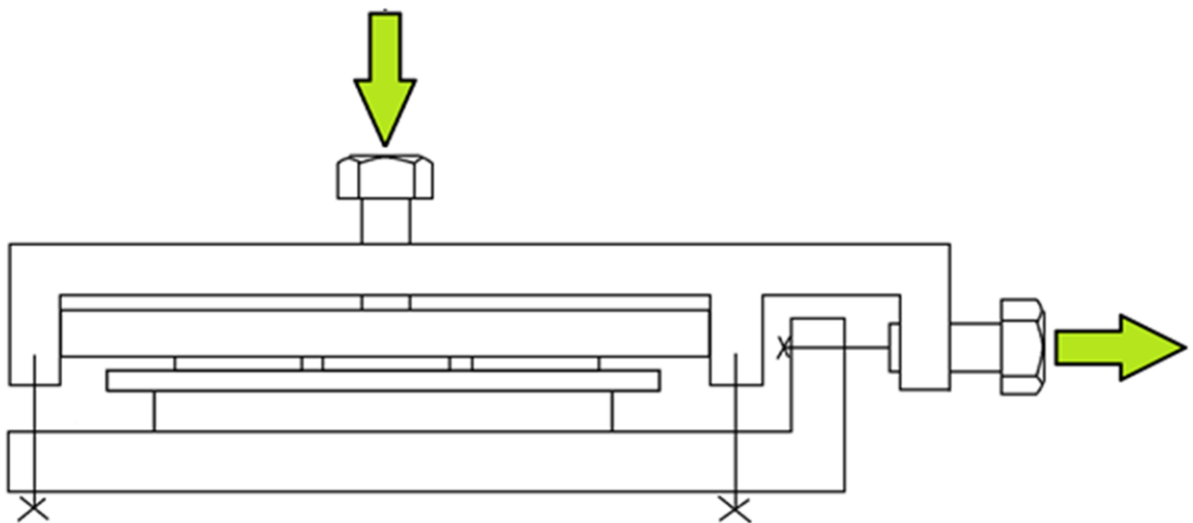


Figure 19: Scheme of concept 5, top view

Disadvantages of wires are their eigenfrequencies. Some modal shapes are just wire vibrations, which are set by their length, diameter, material behaviour and pre-stress.

It is important to tune these eigenfrequencies far enough from eigenfrequencies caused by friction material. It can be done by changing their geometry and Young's modulus. If the pad is well positioned, all axial wires would have the same preload and they would have the same natural frequencies

Another disadvantage is simplification of the tangential force, which is not circumferential, but only straight. Modal sensitivity of this concept has a priority over real clamping. Same as for the other concepts, this affect the contact pressure distribution.

The first revision of this concept was presented with additional plate between caliper half and brake pad. On this plate, there are short extrusions corresponding to


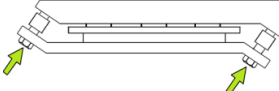
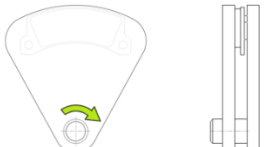
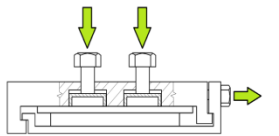
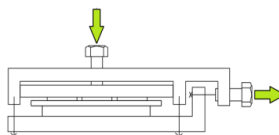
the hydraulic pistons and two longer extrusions corresponding to the caliper pins, so this part is the only one unique part for each pad size. The plate is led by the grooves and it is driven by only one screw. Advantage is obvious, axial preloading with one screw is easy. This revision was set with washer force sensors, mounted under nuts.

There are two main ways how to measure preload forces – the first one is to place sensors between screws and reaction points. Then it is pressed with increasing preload. The second way is to mount tensometers right on the wires.

4.8 Concepts evaluation

For future work, it is necessary to judge the importance of all advantages and disadvantages. These concepts are purposely very different to present as much approaches as possible, so the expected solution is a mixture of several concepts. Positives and negatives are summarized in table 1.

Table 1 Concepts comparison

Concept	+	-
1 	Simple prestressing High repeatability	Simplified tangential force, Tangential force is function of pad thickness
2 	Simple prestressing High repeatability Force sensors with predictable behaviour	Simplified tangential force, Too stiff in tangent direction
3 	The most real force introduction Shear modes in modal analysis	The heaviest one, Damping in the pin
4 	Imitation of calipers with various piston diameter	Simplified tangential force
5 	The most sensitive to friction material attributes, Compact, very stiff assembly	Simplified tangential force

For continuation of this thesis, concepts 2, 3 and 5 were selected as the most likely ones to succeed, because they have some interesting features and less cons than concepts 1 and 4. It was necessary to develop simplified CAD models and then check their behaviour in FE analysis. Especially contact pressure distribution and sensitivity to lining material changes in modal analysis, which is all described in chapter 5.

5 Determination of selected concept

Chapter four was mostly a discussion about benefits and handicaps of developed concepts. Selected concepts were designed in Creo Parametric software and they were created with the aim of resolving the technological design. The first models were just simple thick plates of steel with different types of clamping. It was necessary to verify functionality of these ideas.

This chapter is devoted to development of concept 2, 3 and 5 FE models. Exploration of their pressure distribution and especially modal shapes was necessary for decision of future work.

5.1 Brake pad test models

The universality of the test rig is ensured by using two differently sized brake pads. Each concept was assembled with a smaller pad (figure 17), originating from the two piston caliper and a bigger pad, originating from six piston caliper (figure 18). Coordinate systems used in analysis are shown in these figures.

The first step was to make 3D models of the brake pad with defined material properties. Brake pad consists of two main parts: steel backplate and lining part. As shown in table 2, these materials have significantly different properties.

Table 2 Material properties

Lining material			Steel		
Property	Value	Unit	Property	Value	Unit
ρ	2.7	g/cm ³	ρ	7.8	g/cm ³
E_1	13042	MPa	E_1	$2.1 \cdot 10^5$	MPa
E_2	13042	MPa	E_2	$2.1 \cdot 10^5$	MPa
E_3	11623	MPa	E_3	$2.1 \cdot 10^5$	MPa
ν_{12}	0.158	1	ν_{12}	0.3	1
ν_{23}	0.3	1	ν_{23}	0.3	1
ν_{13}	0.3	1	ν_{13}	0.3	1
G_{12}	5633	MPa	G_{12}	80769	MPa
G_{23}	3261	MPa	G_{23}	80769	MPa
G_{13}	3261	MPa	G_{13}	80769	MPa

As shown, the lining material is orthotropic in contrast with isotropic steel. Also the magnitudes of Young's modulus are nearly twenty times lower. In real brake assembly, this is the most compliant part, so it has a crucial influence on the whole assembly behaviour.

5.1.1 Smaller brake pad

Smaller brake pad, which was used for analysis, comes from fixed two piston caliper used on rear axle. It means that each pad in the brake assembly is pushed against the rotor by one piston. It is 126 mm long and piston diameter is approximately 38 mm. The geometry of the pad is in figure 20.



Figure 20 Brake pad used in two piston caliper

As said in the introduction, results of free modal analysis are strongly different to brake assembly behaviour. Sensitivity of the smaller pad to material changes is shown in table 3. Only one material parameter had been changed and eigenfrequencies were compared to original material. Despite reality, each material parameter was changed separately to investigate sensitivity. Differences higher than 1 % or 10 Hz are highlighted.

Table 3 Smaller brake pad - material changes sensitivity

Mode	Original	Ex, Ey -20%				Ex, Ey -50%			Ez -20%			Ez -50%		
	f [Hz]	f [Hz]	Δ[Hz]	Δ[%]	f [Hz]	Δ[Hz]	Δ[%]	f [Hz]	Δ[Hz]	Δ[%]	f [Hz]	Δ[Hz]	Δ[%]	
7	3223	3072	151	5	2759	464	14	3222	1	0	3219	4	0	
8	4025	3942	83	2	3789	236	6	4022	3	0	4015	10	0	
9	7180	6959	221	3	6390	790	11	7168	12	0	7138	42	1	
10	7260	7135	126	2	6966	295	4	7254	6	0	7240	21	0	

Mode	Original	Gxy -20%				Gxy -50%			Gxz, Gyz -20%			Gxz, Gyz -50%		
	f [Hz]	f [Hz]	Δ[Hz]	Δ[%]	f [Hz]	Δ[Hz]	Δ[%]	f [Hz]	Δ[Hz]	Δ[%]	f [Hz]	Δ[Hz]	Δ[%]	
7	3223	3164	59	2	2994	230	7	3185	38	1	3087	136	4	
8	4025	3920	105	3	3752	273	7	3933	92	2	3712	313	8	
9	7180	7001	179	2	6575	606	8	7009	172	2	6624	557	8	
10	7260	7224	36	1	7185	76	1	7106	154	2	6743	517	7	

Frequencies are nearly constant when changing Young's modulus in axial direction (E_z). Practically it means impossibility of this parameter calculation from free modal analysis results, even though it affects behaviour of brake assembly

significantly. Some modal shapes of smaller pad are shown in figures 21 and 22. It is obvious that clamped brake pad is deformed in another way.

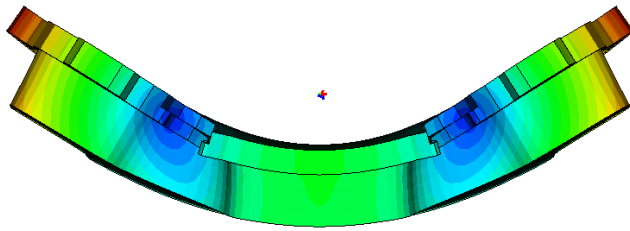


Figure 21 Smaller pad, 1st modal shape - bending

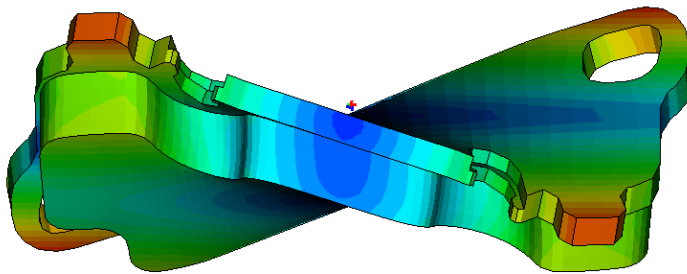


Figure 22 Smaller pad, 2nd modal shape - twisting

5.1.2 Bigger brake pad

Bigger brake pad (fig. 23) is approximately 210 mm long and comes from six piston caliper, used on front axle. It is also a fixed caliper, so the pad is pushed against the rotor by three identical pistons (diameter 3x29mm).



Figure 23 Brake pad used in six piston caliper

On following figures (24-26), some modal shapes of bigger pad are shown.

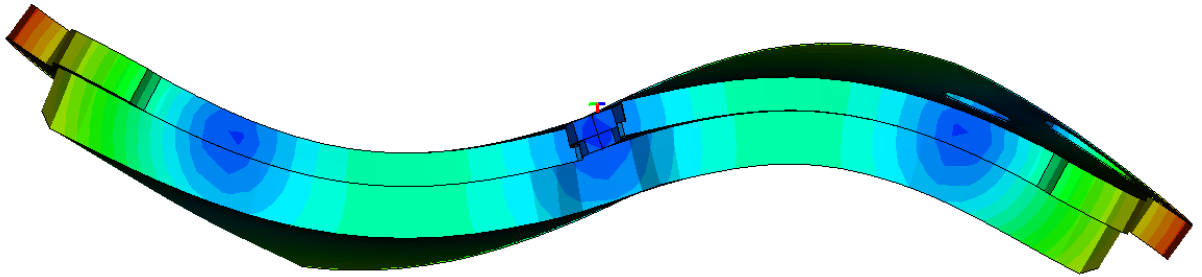


Figure 24 10th modal shape - bending

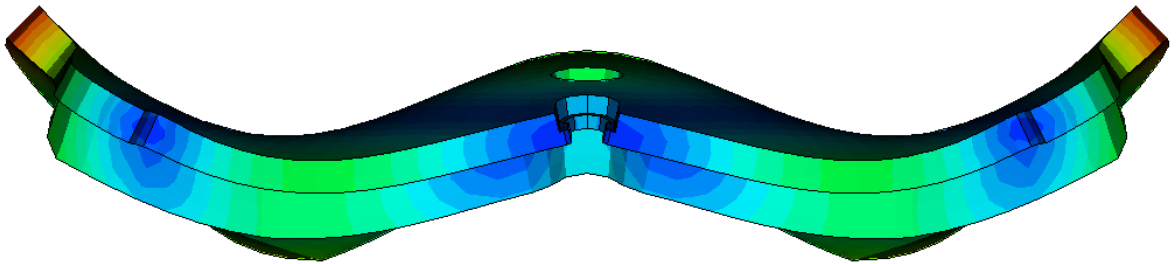


Figure 25 12th modal shape - bending

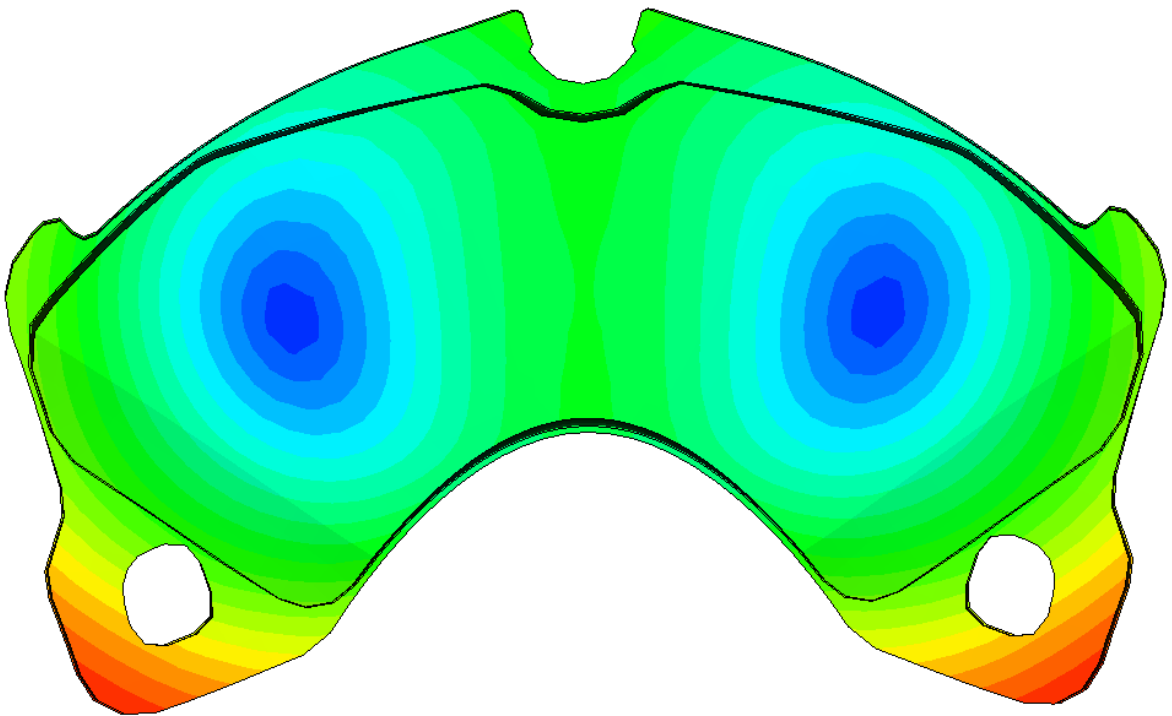


Figure 26 13th modal shape – bending in plane

Table 4 Bigger brake pad - material changes sensitivity

Mode	Original	Ex, Ey -20%			Ex, Ey -50%			Ez -20%			Ez -50%		
	f [Hz]	f [Hz]	Δ [Hz]	Δ [%]	f [Hz]	Δ [Hz]	Δ [%]	f [Hz]	Δ [Hz]	Δ [%]	f [Hz]	Δ [Hz]	Δ [%]
7	1183	1118	65	6	1005	179	15	1183	0	0	1183	0	0
8	1608	1604	4	0	1597	12	1	1608	0	0	1607	1	0
9	2996	2863	133	4	2619	377	13	2995	1	0	2994	2	0
10	3349	3322	27	1	3266	82	2	3347	2	0	3343	6	0
11	4708	4657	51	1	4559	149	3	4705	3	0	4698	9	0
12	5203	5021	182	3	4660	543	10	5202	1	0	5199	4	0
13	5509	5478	31	1	5429	81	1	5509	0	0	5509	0	0
14	6569	6489	80	1	6319	250	4	6566	3	0	6559	10	0
15	6890	6709	181	3	6359	531	8	6889	2	0	6884	6	0
16	7288	7056	232	3	6635	653	9	7285	3	0	7279	9	0
17	8105	8016	89	1	7794	311	4	8102	3	0	8095	10	0
18	8872	8632	240	3	8205	667	8	8869	3	0	8862	9	0
19	9161	8950	211	2	8556	605	7	9156	5	0	9143	18	0

Mode	Original	Gxy -20%			Gxy -50%			Gxz, Gyz -20%			Gxz, Gyz -50%		
	f [Hz]	f [Hz]	Δ [Hz]	Δ [%]	f [Hz]	Δ [Hz]	Δ [%]	f [Hz]	Δ [Hz]	Δ [%]	f [Hz]	Δ [Hz]	Δ [%]
7	1183	1182	1	0	1180	3	0	1179	4	0	1169	15	1
8	1608	1536	73	5	1402	206	13	1590	18	1	1545	64	4
9	2996	2992	4	0	2983	13	0	2965	31	1	2886	110	4
10	3349	3243	106	3	3037	312	9	3310	39	1	3213	136	4
11	4708	4632	76	2	4482	226	5	4648	60	1	4506	202	4
12	5203	5194	9	0	5174	29	1	5132	71	1	4959	244	5
13	5509	5498	12	0	5476	33	1	5506	3	0	5499	11	0
14	6569	6489	79	1	6350	219	3	6495	74	1	6320	249	4
15	6890	6840	50	1	6740	150	2	6807	83	1	6607	284	4
16	7288	7237	52	1	7136	152	2	7199	89	1	6982	306	4
17	8105	8012	93	1	7850	255	3	8008	97	1	7784	321	4
18	8872	8831	41	0	8750	122	1	8738	134	2	8435	436	5
19	9161	9082	79	1	8928	232	3	9022	139	2	8699	462	5

As shown in the table 4, eigenfrequencies change with E_z (Young's modulus in axial direction) only very slightly. In fact, this material parameter is important in real brake assembly behaviour.

5.2 Geometry development

All the concepts have some identical symptoms in modal analysis. Brake pad in the centre of assembly acts like a spring between two oscillating masses. Deformations of these components makes identification of brake pad behaviour more complicated. Some undesired modal shapes of concept 5 are shown in figures 27, 28, and 29.

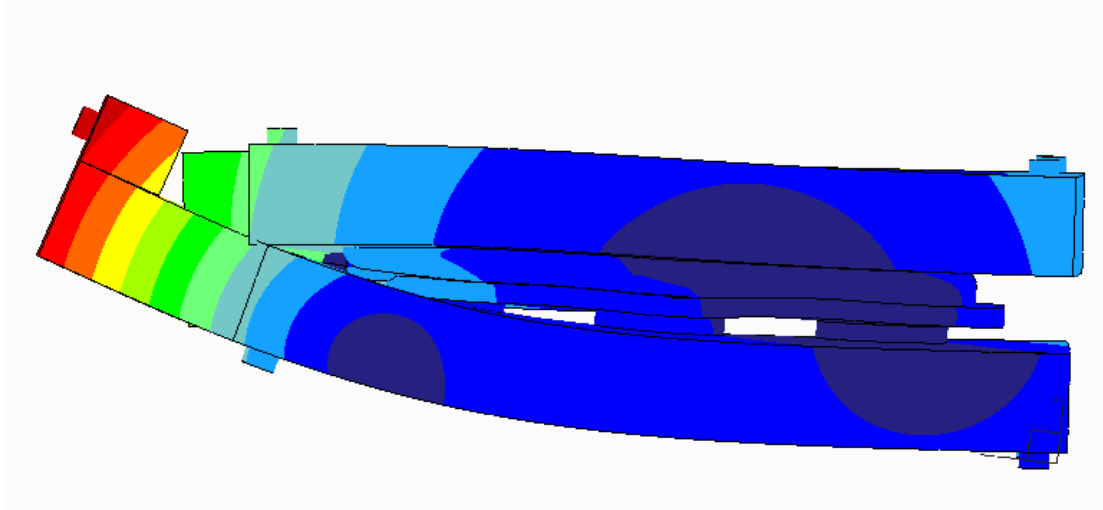


Figure 27 First bended shape of the rig

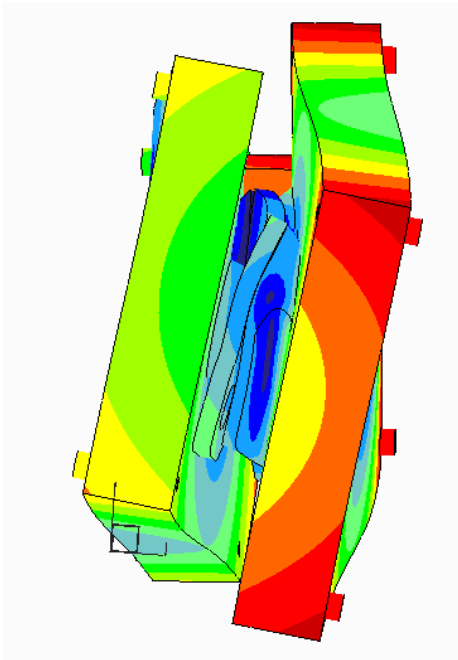


Figure 28 twisted shape of the rig

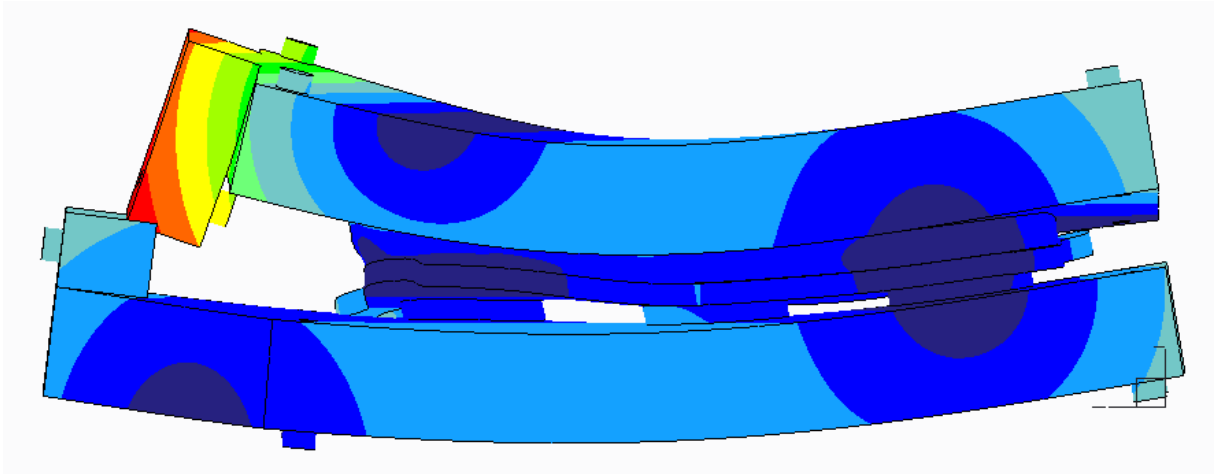


Figure 29 Second bended shape of the simple rig

To avoid this fact, all the concepts were designed to be stiffer. The top view shows the bow shape to reduce bending of concept 2 and 5 (fig. 30 and 36). The other problematic deformations are mitigated by ribs on the front and back side.

5.2.1 Concept 2

Geometry of concept 2 with bigger pad is shown in figure 30. Exploded parts are in figure 31. Principle described in chapter 4.5 is not changed.

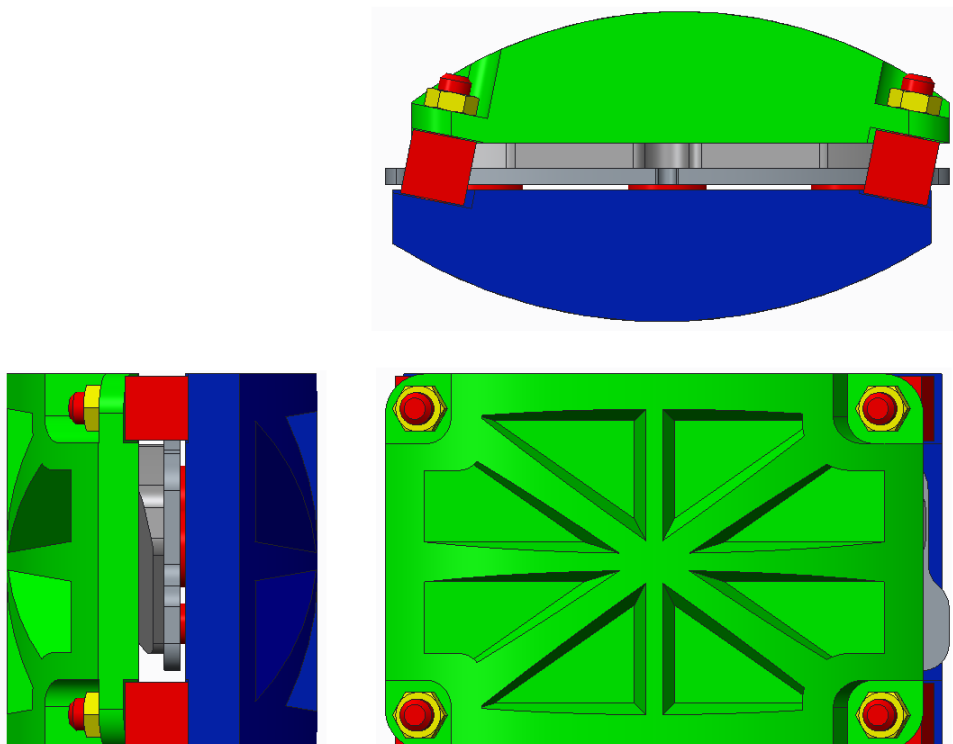


Figure 30 Concept 2

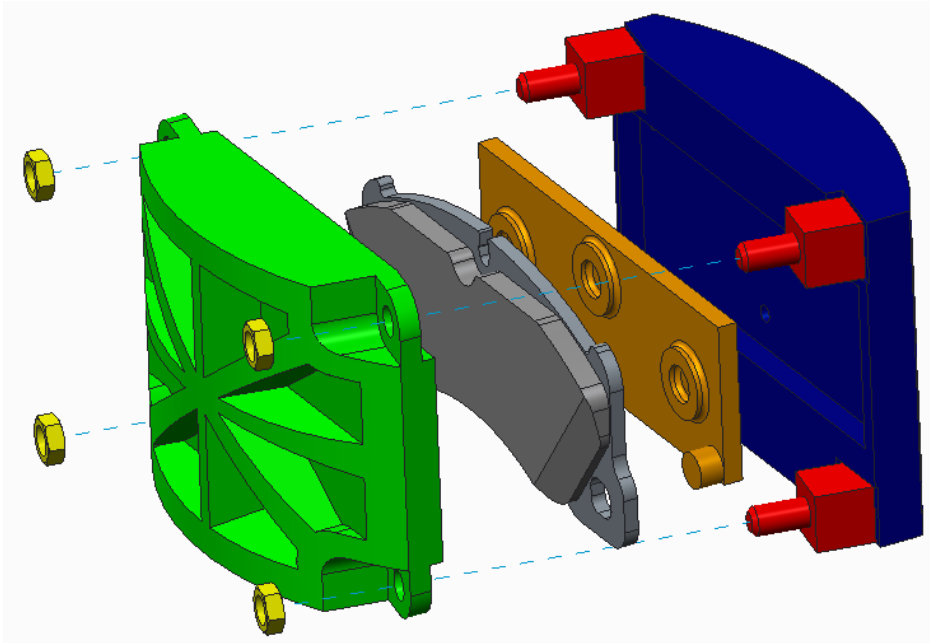


Figure 31 Concept 2, exploded view

For this sensitivity analysis, all contacts were tied, so that the damping influence of contacts was neglected. This concept proved to be sensitive to Young's modulus in axial direction (E_z). On the other hand, changing material parameters in remaining directions does not change eigenfrequencies enough. Important modes are listed in table 5, one of these mode is shown in figure 32.

Table 5 Concept 2 sensitive modes

Mode	Shape	Frequency [Hz]	Δ [Hz]	Mat. parameter change 20%
11	Axial	2262	107	E_z
13	Axial	3035	282	E_z

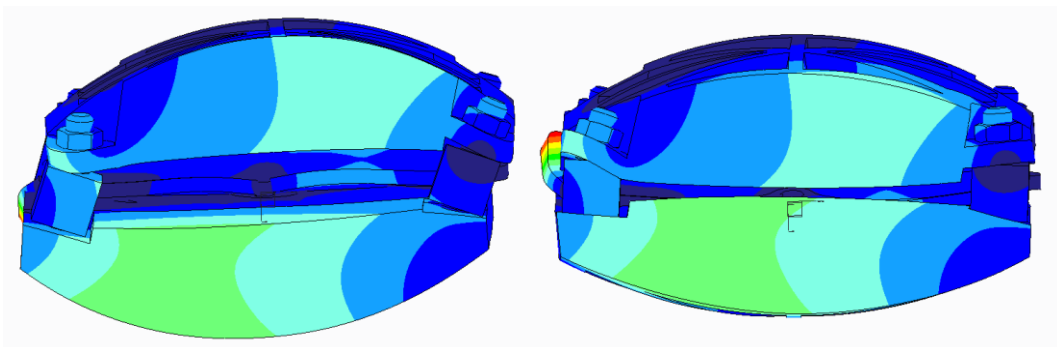


Figure 32 Mode sensitive to Young's modulus in axial direction (13th mode)

5.2.2 Concept 3

Concept 3 has a unique design because of the pin constraint. Ribs are situated to make the rig stiffer and to prevent large deforming of both halves (figures 33, 34). Principle described in chapter 4.6 is modified by prestressing realised by wires. Wire for tangential preloading located on the side proved to be problematic, because it needs a lot of mass with limited possibilities of reinforcement.

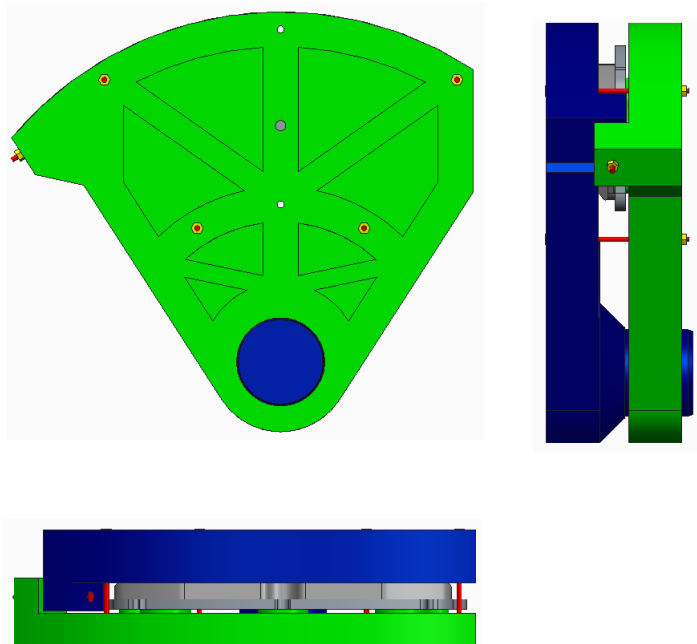


Figure 33 Concept 3

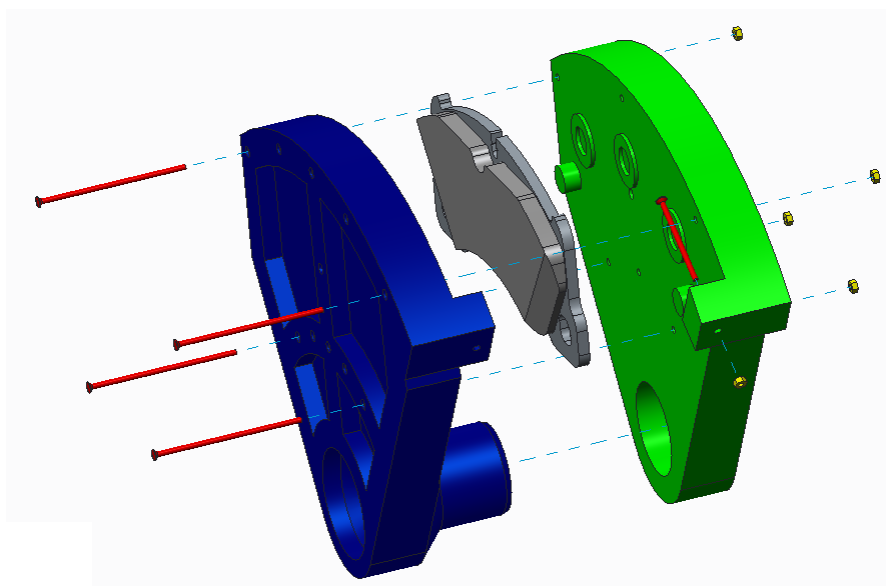


Figure 34 Concept 3 with bigger pad, exploded view

The huge problem of this design is insensitivity to material changes. Table with shear mode information (table 6) and figures with its shape (figure 35) are shown below. This shear mode doesn't have large difference of frequency, but the shape is very similar to real brake assembly behaviour.

Table 6 Concept 3 sensitive mode

Mode	Shape	Frequency [Hz]	Δ [Hz]	Mat. Parameter change by 20%
8	Shear	3029	82	G_{xz} , G_{yz}

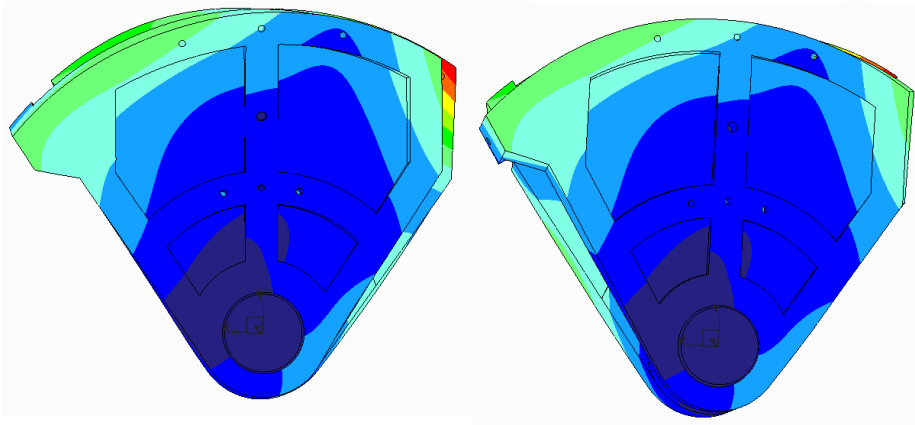


Figure 35 Shear deformation, 8th mode

5.2.3 Concept 5

This concept puts the greatest emphasis on sensitivity of material parameters changes. Constraints are as compliant as possible, total mass is also reduced to possible minimum. Geometry is shown in figure 36, detailed parts are in figure 37.

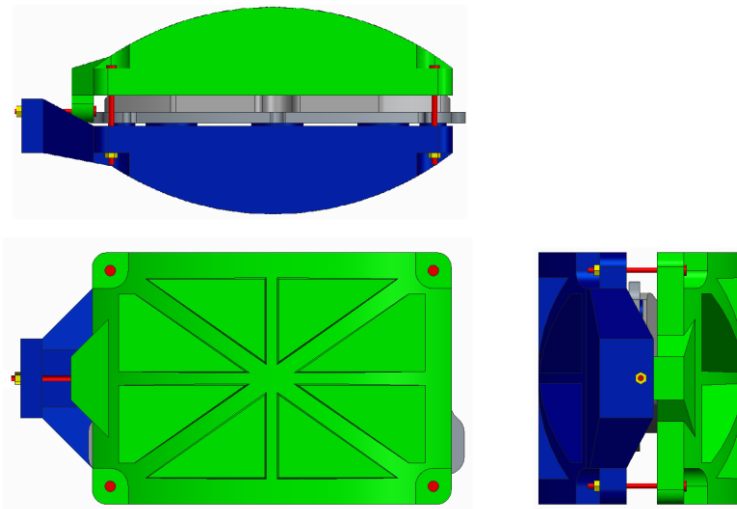


Figure 36 Concept 5

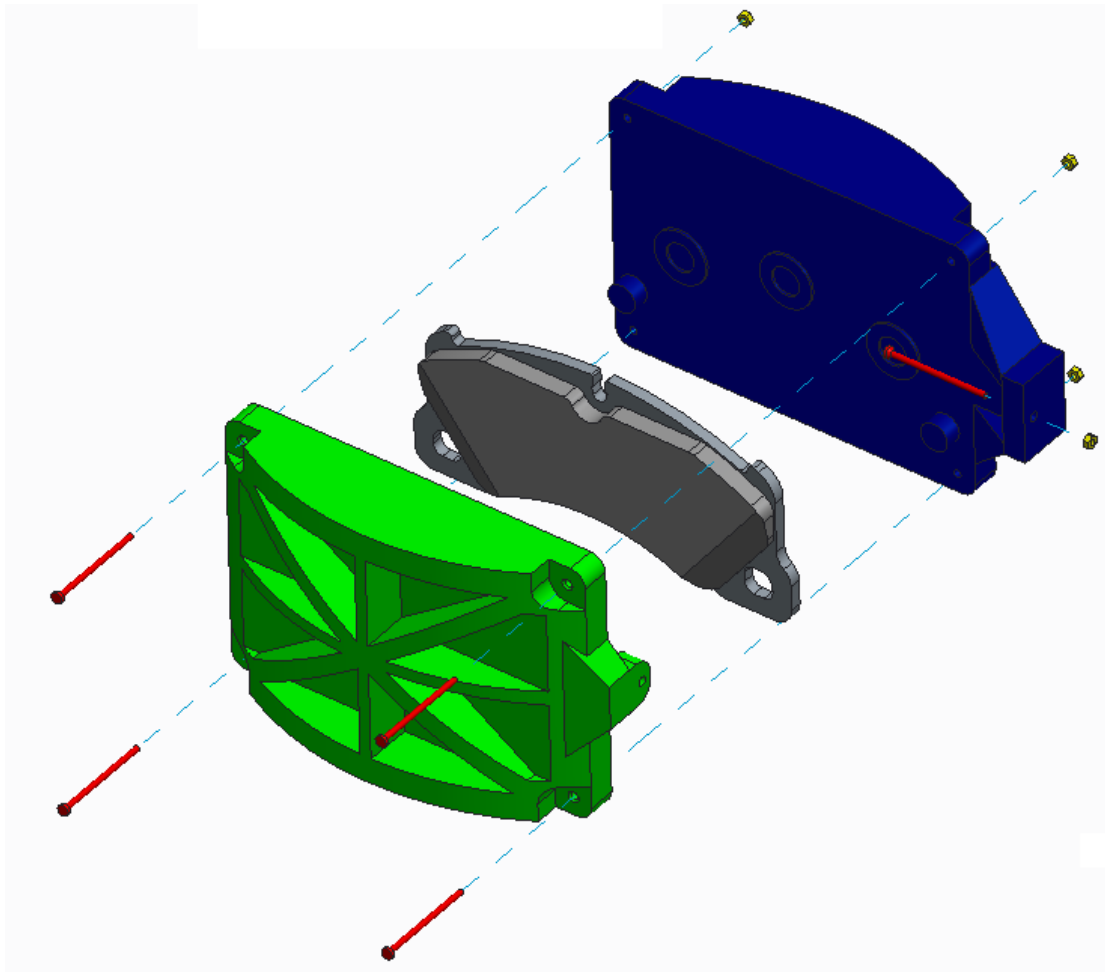


Figure 37 Concept 5 with bigger pad, exploded view

This concept is really the most sensitive to lining material parameter changes. Especially changing of G_{xz} and G_{yz} caused significant frequency changes. On the other hand, modal shapes are not similar to real conditions. Table with interesting modes and their shapes is shown below.

Table 7 Concept 5 sensitive modes

Mode	Shape	Frequency [Hz]	Δ [Hz]	Mat. parameter change 20%
7	swinging	1161	107	G_{xz}, G_{yz}
11	bending	3093	146	G_{xz}, G_{yz}
12	torsion	3267	155	G_{xz}, G_{yz}

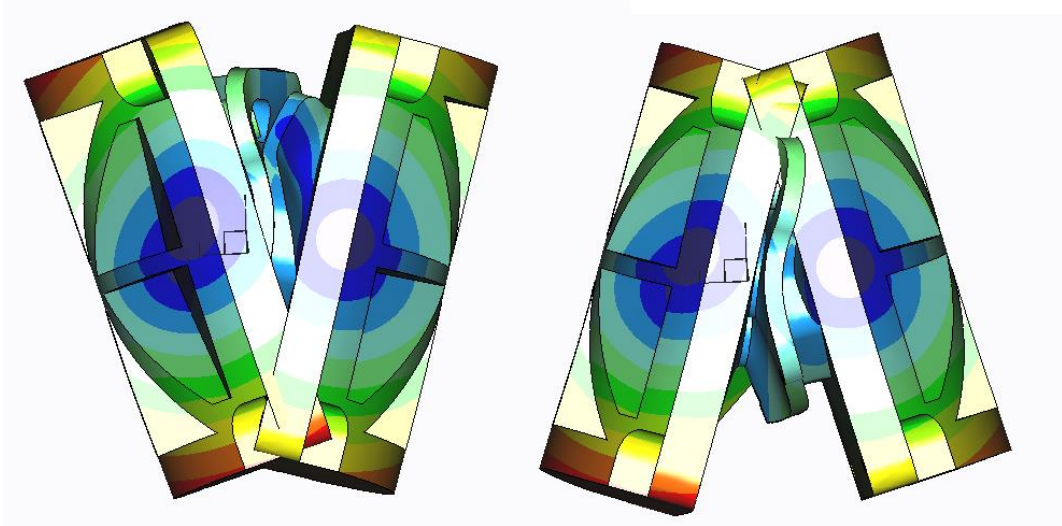


Figure 38 Swinging of the rig halves, 7th mode

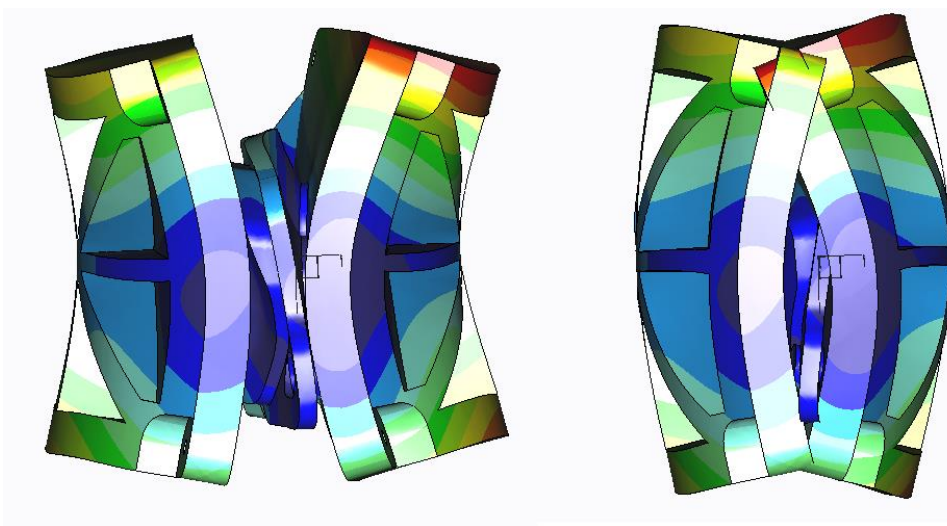


Figure 39 horizontal bending, 11th mode

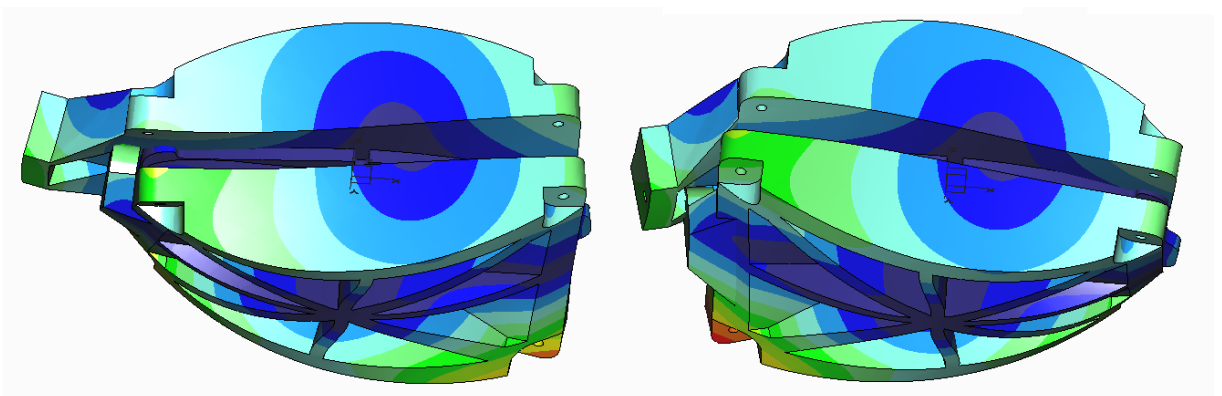


Figure 40 Torsion, 12th mode

5.4 Final concept geometry

Cylindrical constraint has proven to be important, but the concept number 3 had very low sensitivity. For continuing of the work, it was necessary to combine advantages of concepts 3 and 5, and to suppress their weaknesses. Final geometry is a hybrid of these two concepts with some new features. The biggest change is a move of tangential preloading wire to the top of assembly. The design became more symmetric, and it positively affected modal shapes.

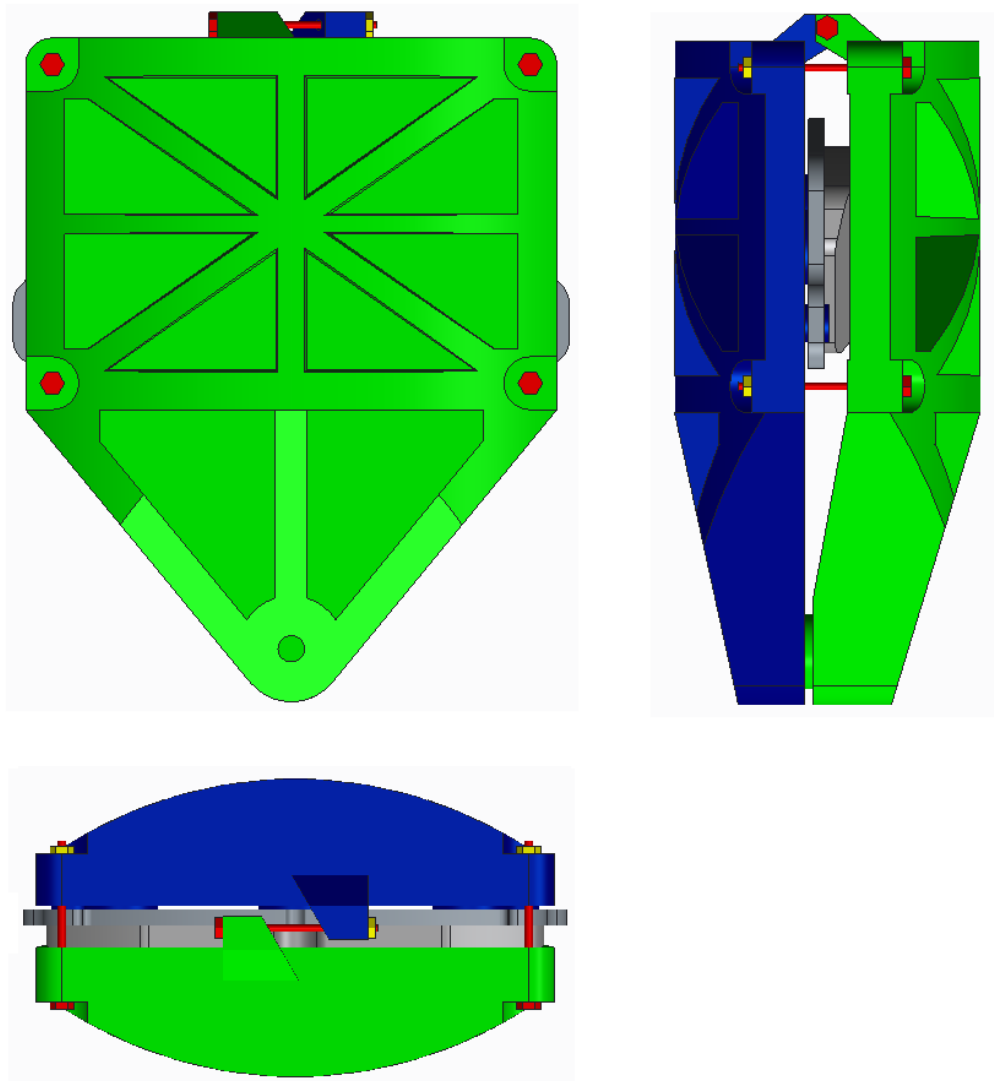


Figure 41 Final geometry for FEM simulation

Table 8 Parts list of final concept

Title	Material	Quantity
Front half	Steel	1
back half	Steel	1
wire	Steel	5
nut	Steel	5
Backplate	Steel	1
Lining material	Composite	1

All the wires have the same length 50 mm and diameter 3 mm. It is useful for manufacturing, but the wires have different preload magnitudes, so there they caused eigenfrequencies of the rig in some range. They vibrate like the strings in musical instruments. This range should be as minimal as possible to enable measuring of eigenfrequencies affected by lining material. Parts of this assembly are shown in exploded view (figure 42).

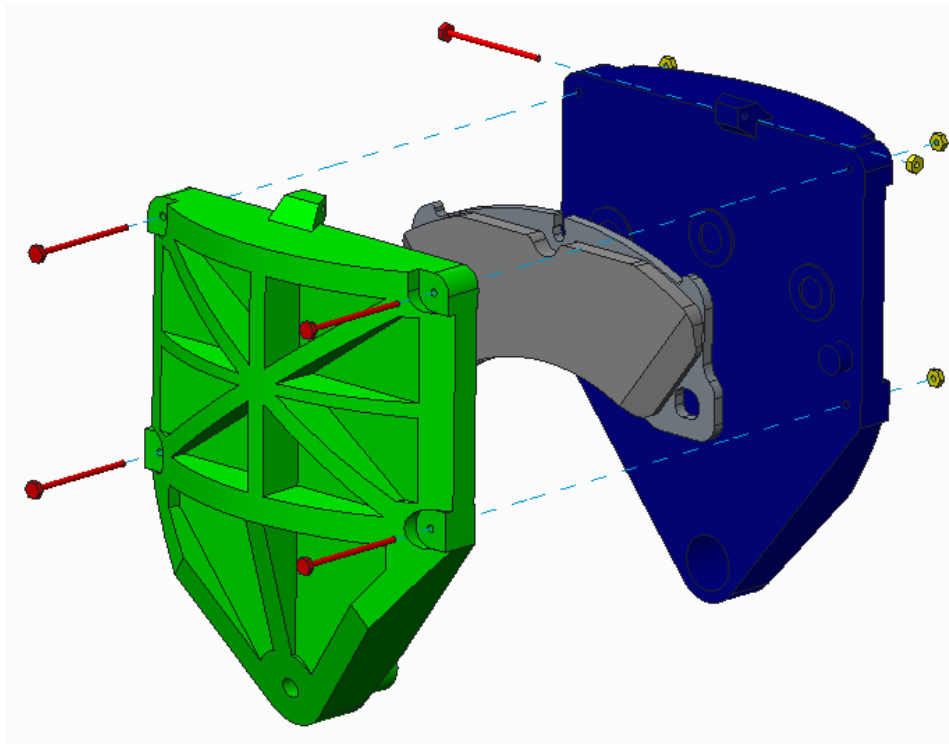


Figure 42 Final geometry for FEM simulation, exploded view

The back half of the rig (blue one) has machined extrusions of pistons and guiding pins. This part must be unique for each brake caliper. Even though it is more expensive than embedded plate with pistons and pins extrusions, it provides better repeatability with less damping. Flat surfaces between the ribs are suitable for accelerometers placement.

6 FEM analysis

Foregoing analyses were computed in Creo Parametric 2.0 software to reduce the preparation time. Models were simplified and results were only for assessment of function. Final concept was pre-processed in ANSA v15.2.0 software and processed in Abaqus 6.13. All results were post-processed in METAPost v15.2.0.

All the analyses consist of static nonlinear step and dynamic step. The static one includes introducing of preloading forces and analysis of pressure distribution. The dynamic one is modal analysis.

Nominal pressure for analyses was 1 MPa (10 Bar), but sensitivity analyses were done also for 0.5 MPa and 2 MPa.

During these simulations, mass of accelerometers and some technological issues, like the fillets, were neglected. It means that results are not exactly the same as expected results of experimental analysis. Main purpose is to verify the correctness of selected approach.

6.1 FE model

6.1.1 Mesh properties

Assembly consists of tetrahedron, pentahedron, and hexahedron elements. Lining material is meshed by hexahedron elements, backplate is meshed by pentahedron elements and other parts are meshed by second order tetrahedron elements. As shown in table 9, smaller pad consist of higher amount of elements than bigger pad. It provides better stability to smaller pad analysis. Simulation of assembly with bigger pad had satisfactory stability even with rough meshed pad.

Table 9 Elements quantity

	smaller pad	bigger pad
tetrahedrons ²	120 912	120 912
pentahedrons	168	182
hexahedrons	8920	4222

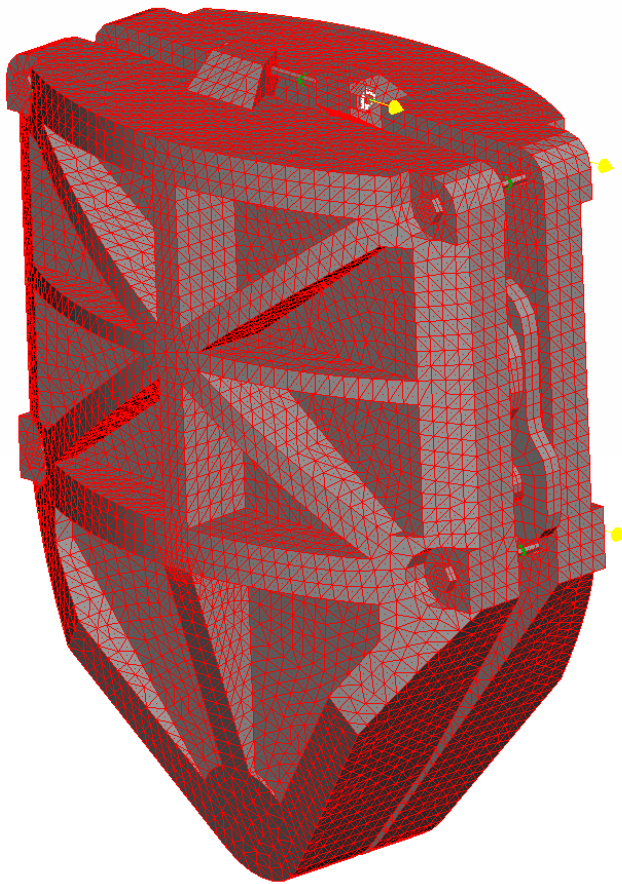


Figure 43 Meshed assembly

6.1.2 Constraints

The assembly consists of 14 parts, which are connected by 3 different constraints. These constraints are shown in figure 41 and described below.

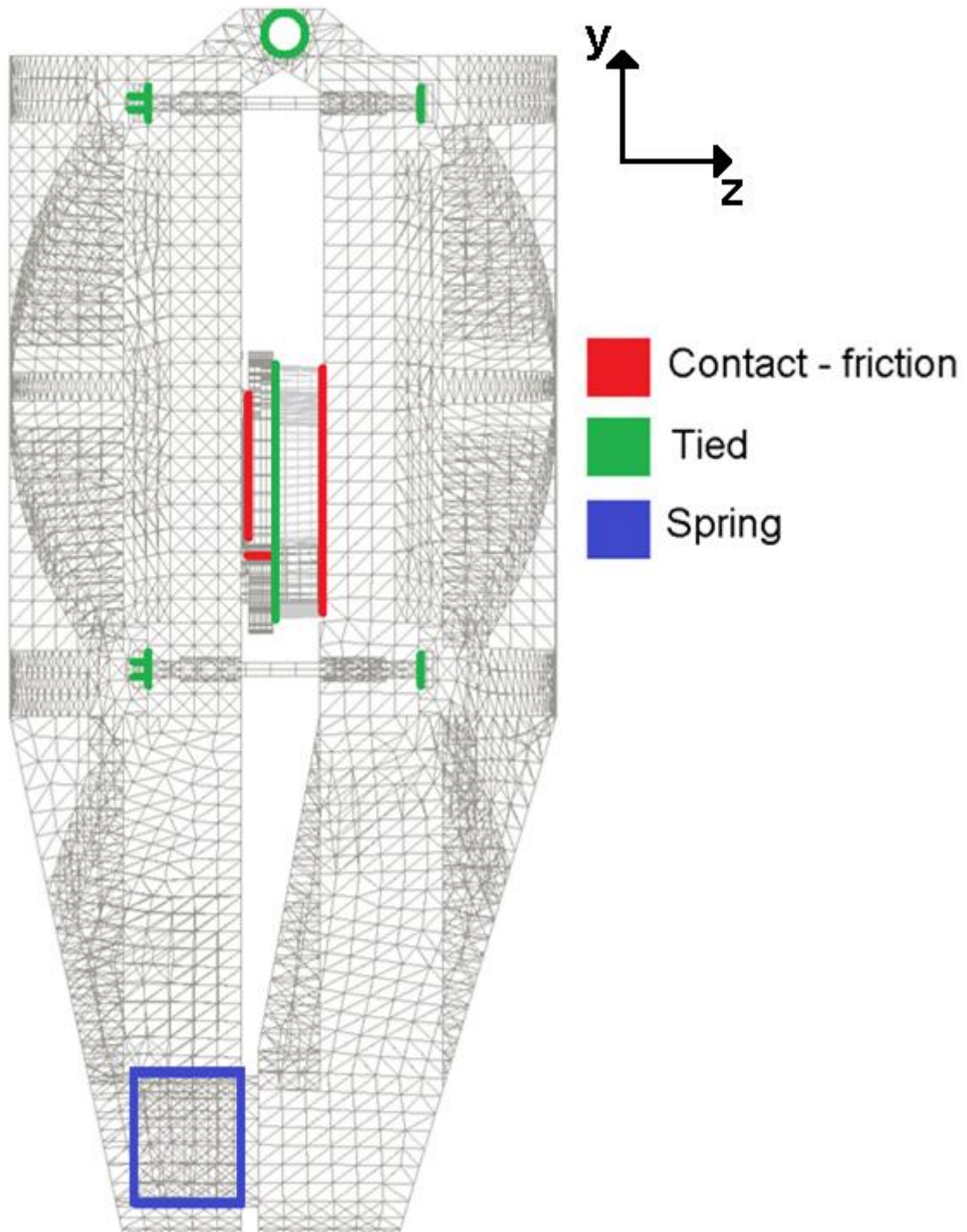


Figure 44 Constraints in the model

The very special is pin between main halves. It must allow translational motion in axial direction and mutual rotational motion. This is achieved by radially arranged beams (figure 45) on both parts, connected by spring with different stiffness for each direction. Table of spring properties is shown below (table 10). Damping of the pin is avoided.

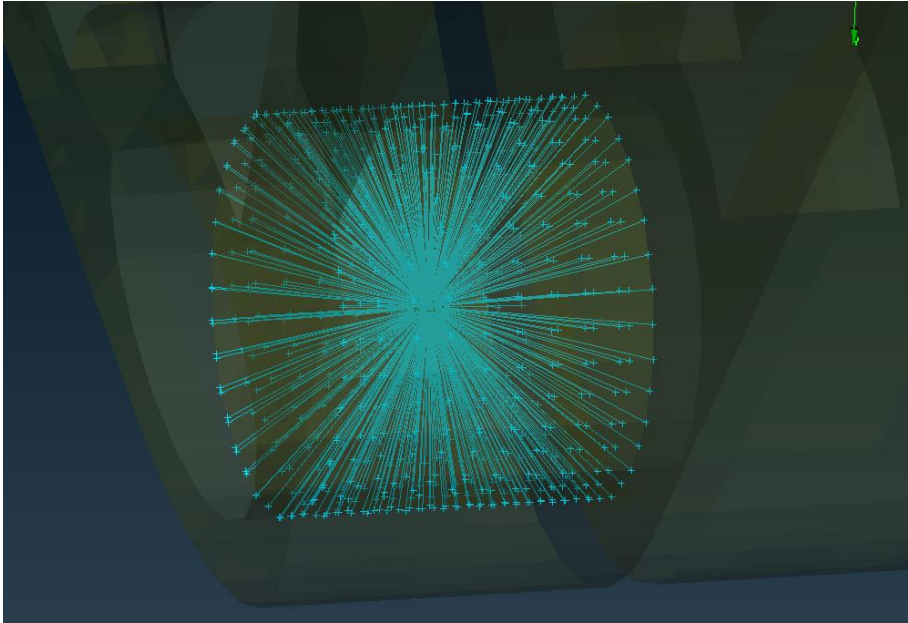


Figure 45 Radially arranged beams

Table 10 Spring properties

Stiffness	Direction	Magnitude
S ₁	x	1e ⁷ [N/m]
S ₂	y	1e ⁷ [N/m]
S ₃	z	0
S ₄	rotation x	1e ⁹ [Nm/Rad]
S ₅	rotation y	1e ⁹ [Nm/Rad]
S ₆	rotation z	0

Some of surfaces contacts are solved by nonlinear contact analysis with specific contact of friction. These are the contacts, where the possibility of slippage exists and pressure distribution is important. Practically, this is applied to all contacts of brake pad with surroundings. List of these constraints with their behaviour is in table 11.

Table 11 Analysed contacts

Contact surface		Coefficient of friction
Linin mat.	Rig	0.4
Backplate	Pistons	0.1
Backplate	Guide pins	0.1

All the other contacts are tied. It means for all wires and nuts contacts, which are expected to be pressured without slippage. This is also applied for friction material and backplate connection. Nodes of surrounding parts are connected together.

6.1.3 Preloading

Every wire is preloaded through the section, as shown in figure 45. They all have diameter 3 millimetres. Maximal pressure 2 MPa on bigger pad variant corresponds to preloading force 1526 Newton on top wires, as shown in figure 46. It means 216 MPa of longitudinal static stress. Magnitude of tangential preloading force corresponds to 40% of axial force and it acts effective braking radius of the pad. True preloading force on tangential wire is lower, because it operates on larger radius. Magnitudes for tangential wires were computed from desired magnitudes on friction surface lever rule. Table 12 shows magnitudes of forces to all configurations.

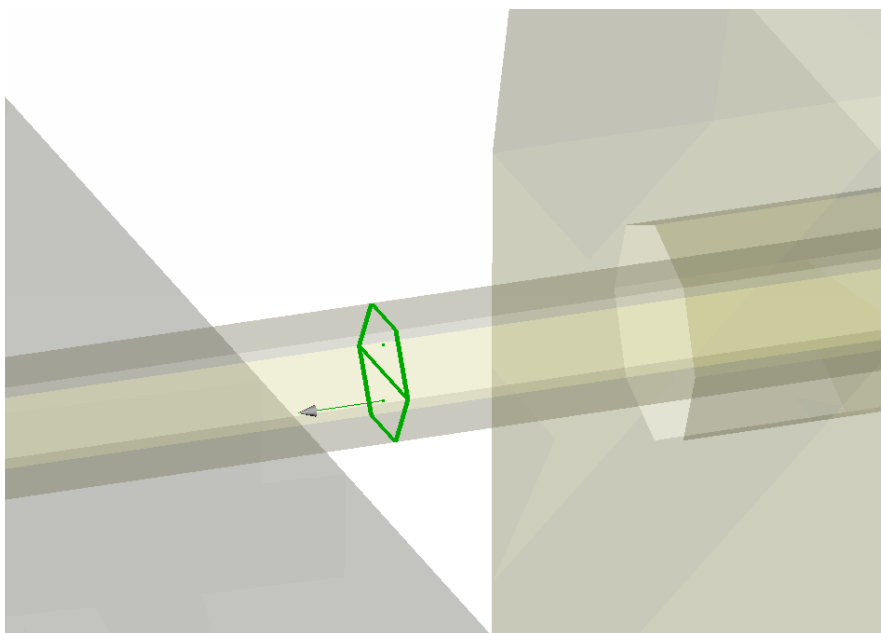


Figure 46 wire section

Table 12 Preloading forces magnitudes

	Smaller pad			Bigger pad		
Pressure [MPa]	0.5	1	2	0.5	1	2
Bottom wires [N]	2x250	2x500	2x1000	2x382	2x763	2x1526
Top wires [N]	2x130	2x260	2x520	2x382	2x763	2x1526
Tangential wire [N]	86	172	344	250	500	1000

As said, brake pad location depends on real brake disc diameter, but position of preloading wires is set without possibility of adjustment. For achievement good pressure distribution on smaller pad, top wires are preloaded less than bottom wires (figure 47). Ratio was set by comparing of the rig pressure distribution with the same result of complex eigenvalue analysis.

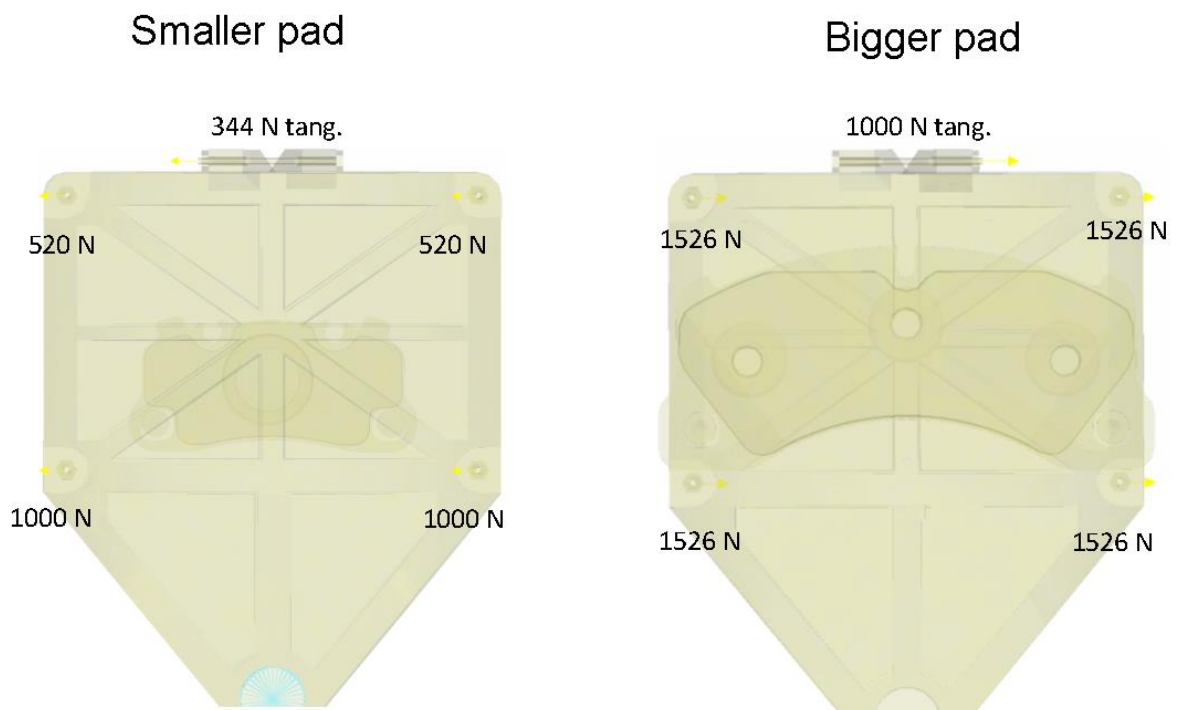


Figure 47 Force magnitudes on all wires for 2 MPa

6.2 Results

Pressure distribution and sensitivity of natural modes are crucial attributes of the rig. For such a wide range of excitation frequencies is probably impossible to have significant changes in all eigenfrequencies. Attention is focused on selected modes, which can enable reverse description of lining material parameters.

6.2.1 Pressure distribution

For right imitation of brake caliper, pressure distribution between lining material and the rig is good index. Tuning was carried out by comparison simulation of pressure distribution in real calipers and rig pressure distribution. It was done by changing ratio between top and bottom wires.

In figures with pressure distribution (figure 48 and 50), blue areas are not pressured. Pistons silhouettes are visible on both pads. Introduction of tangential force can be seen on non-symmetric pressure on lining material edges, where the left edges are more pressured than the right ones.

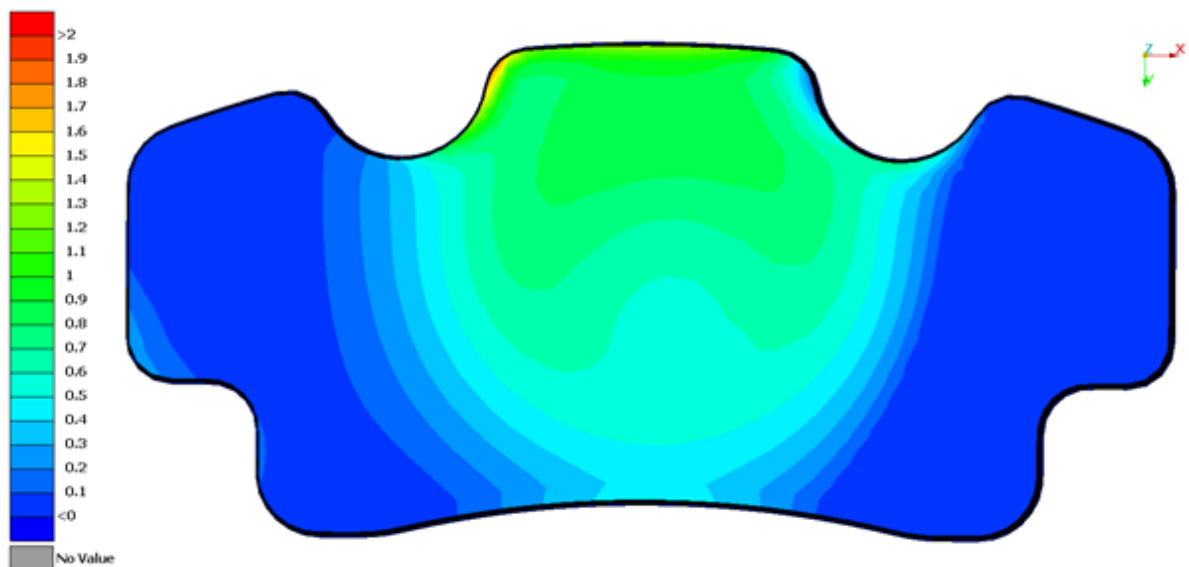


Figure 48 Smaller pad pressure distribution

Figures 49 and 51 with contact status show the areas without slippage (red), area with slippage (green) and areas without contact (blue). Distribution of these areas is dependent on ratio between axial and tangential force, which stays constant for all analyses.

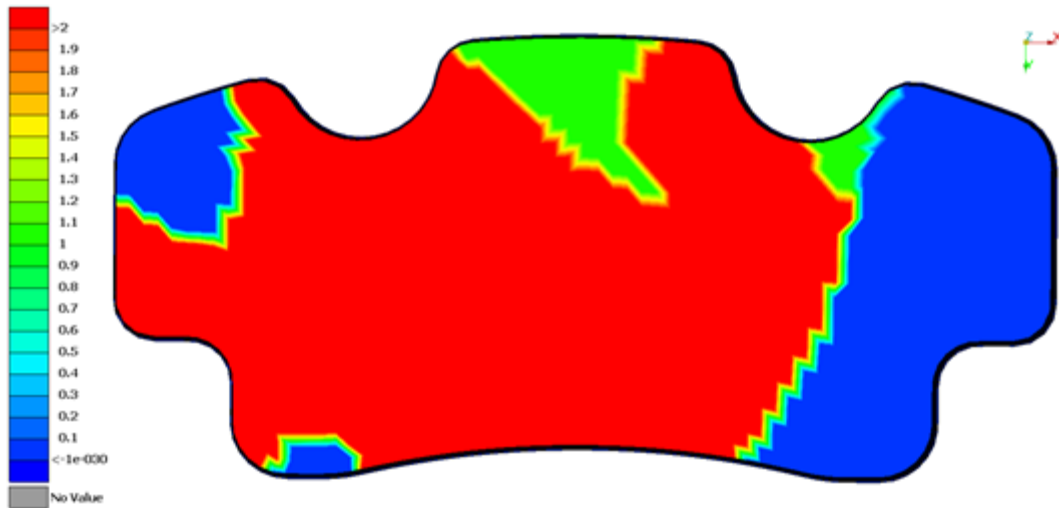


Figure 49 Contact status on smaller pad

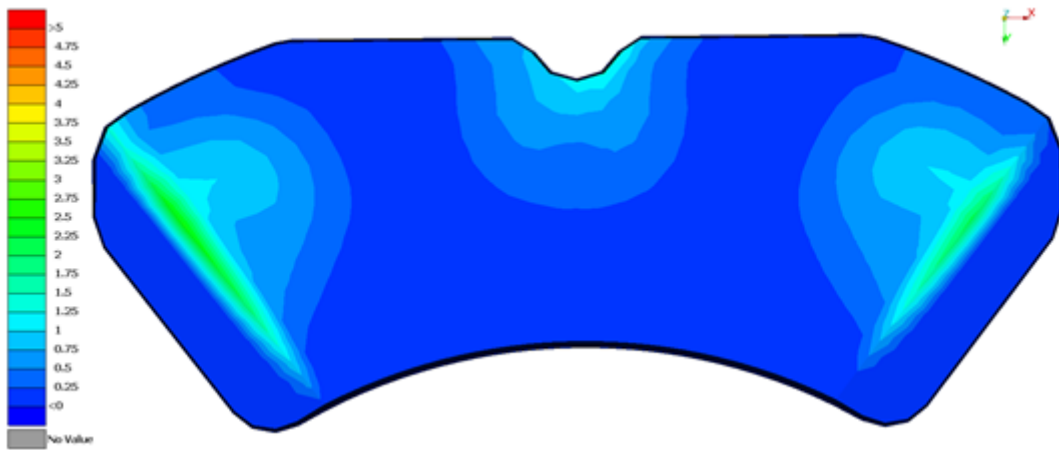


Figure 50 Bigger pad pressure distribution

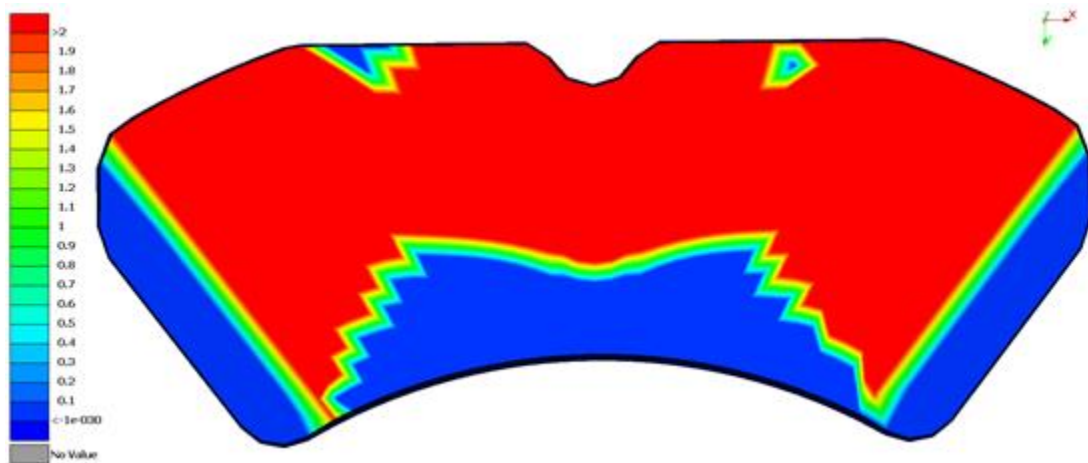


Figure 51 Contact status on bigger pad

6.2.2 Modal shapes, sensitivity with smaller pad

For sensitivity testing, eigenfrequencies were analysed with default lining material properties. Then one of the parameters was decreased by 20% and new eigenfrequencies were compared with the original ones. The same process was repeated for 50% decrease. The best result would be to have each modal shape sensitive to changing only one material parameter.

This kind of analysis was done for preloading pressure of 0.5, 1 and 2 MPa. Some modal shapes are more sensitive only at the specific pressure, the others are not dependent on pressure changes.

List of Interesting frequencies of smaller pad assembly is in table 13. Difference of eigenfrequency corresponds to lining material change 50 %. Figures with shapes are shown below (fig. 52-57).

Table 13 Sensitive modes of the whole preloaded assembly, smaller pad

Mode	Frequency [Hz]	Sensitive to parameter	Δf [Hz]
7	774	Ez	93
8	1127	Ez	102
9	1760	Gxz, Gyz	293
11	2511	Gxz, Gyz	303
15	3609	Ez	128

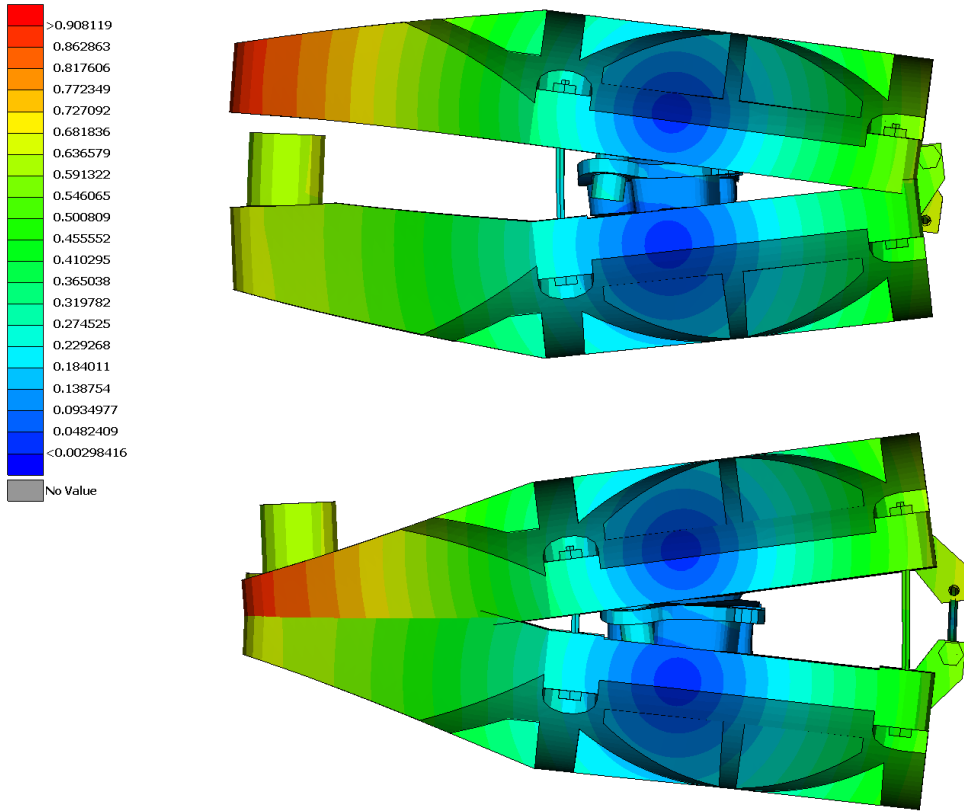


Figure 52 Smaller pad, 7th shape

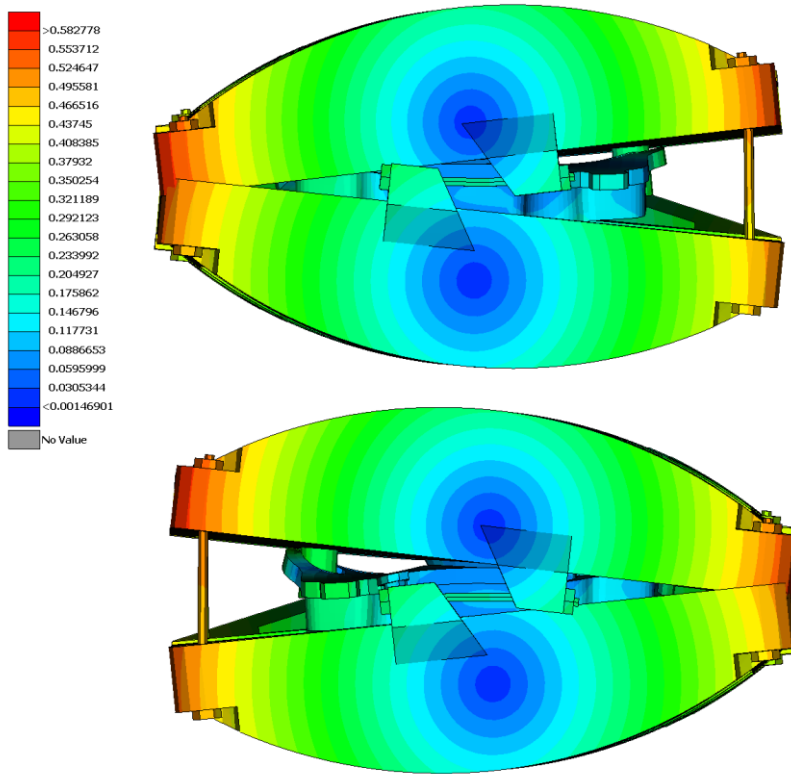


Figure 53 smaller pad, 8th shape

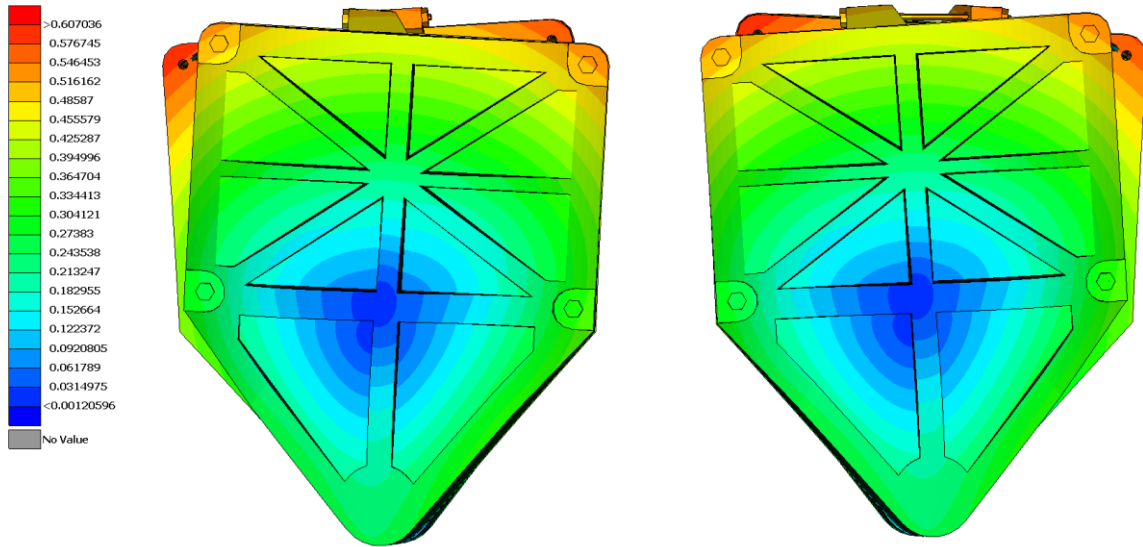


Figure 54 smaller pad, 9th shape – shear mode

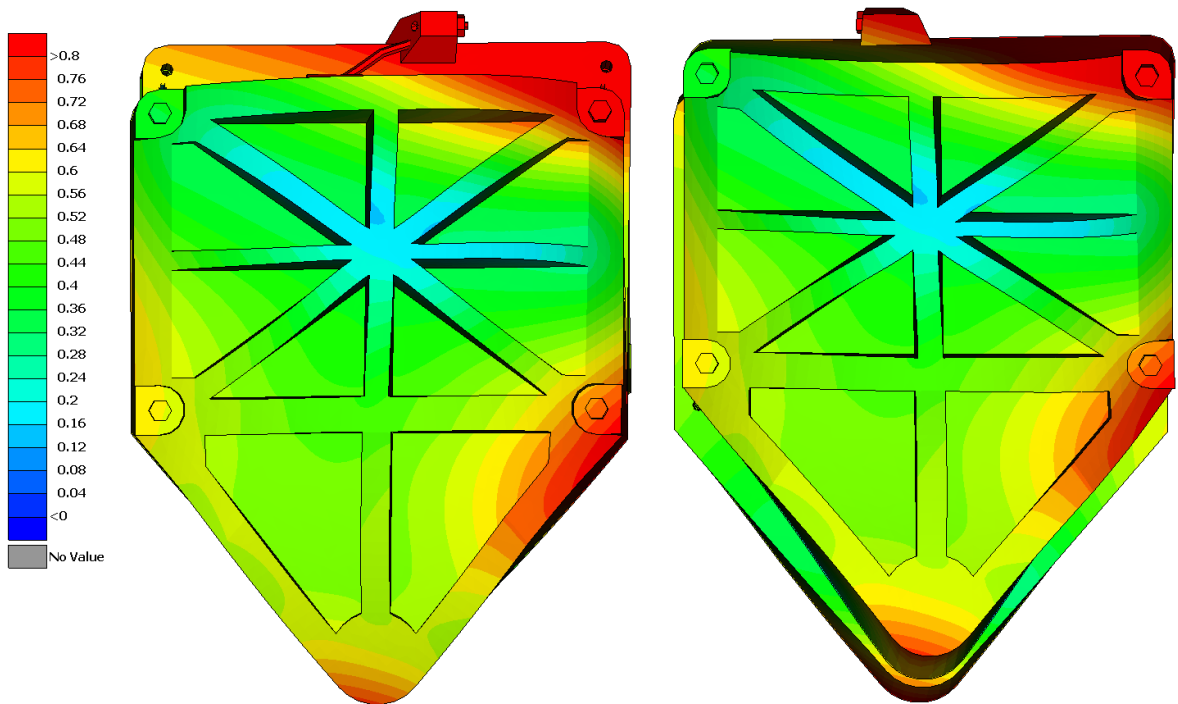


Figure 55 smaller pad, 11th shape

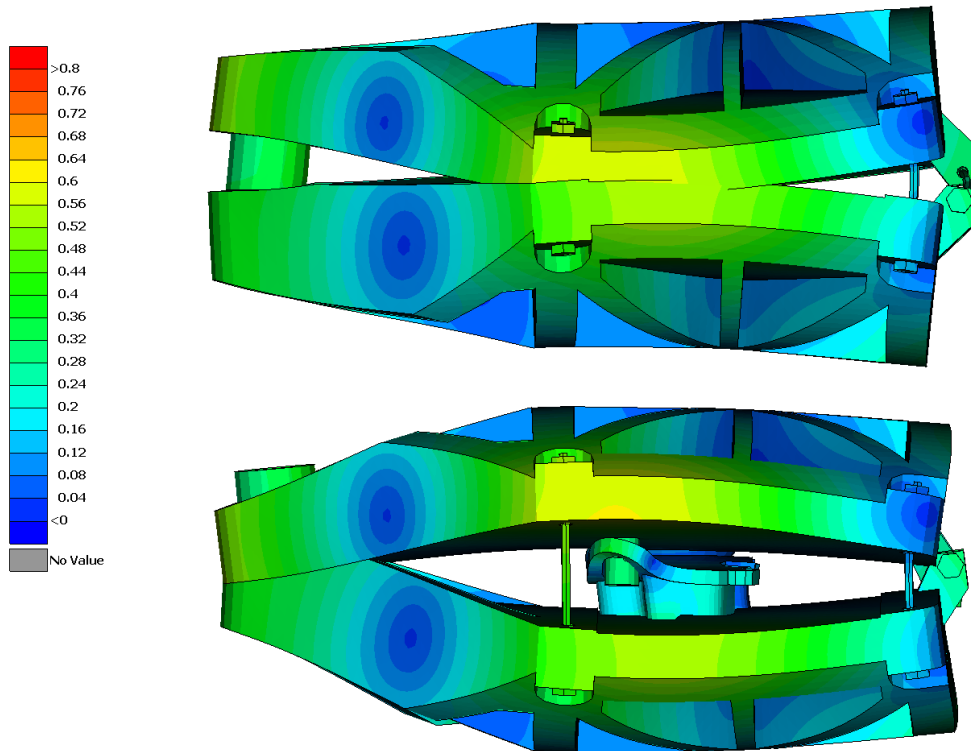


Figure 56 smaller pad, 15th shape

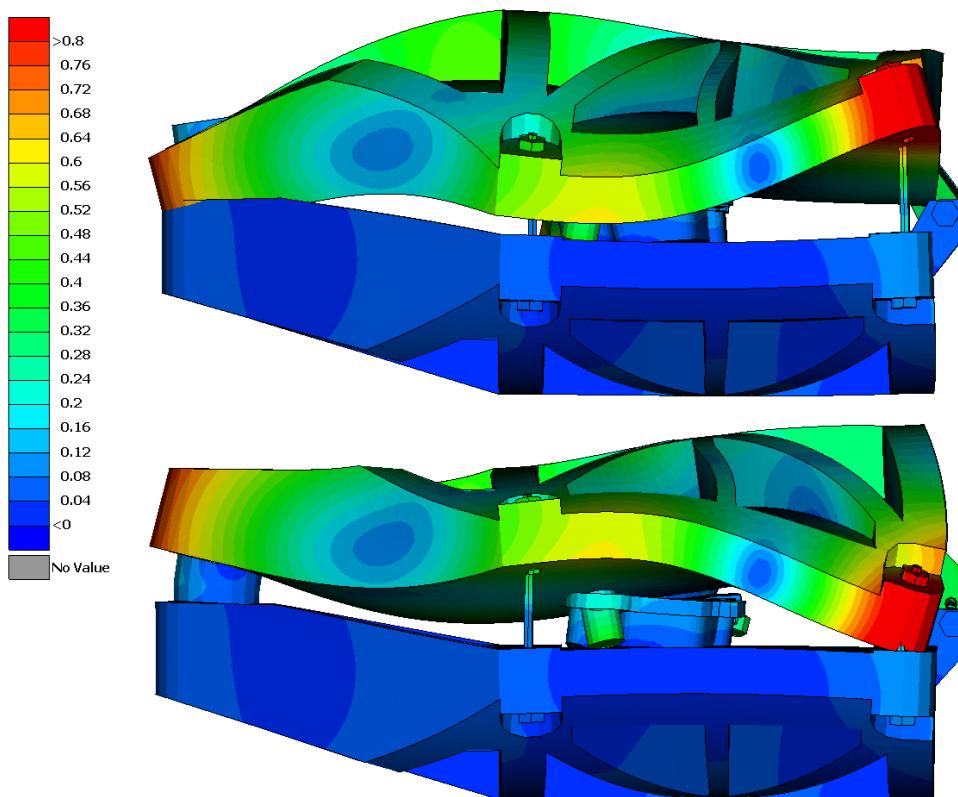


Figure 57 smaller pad, 35th shape

Modes at frequencies higher than 7 kHz are interesting by their sensitivity to all lining material parameters. On the other hand, it doesn't provide information which one of the parameters was changed.

In the figure 58, modal assurance criterion (MAC) matrix for G_{xz} and G_{yz} change 50% is shown. It compares similarity of modal shapes of the rig assembly with original (horizontal axis.) and modified (vertical axis) lining material. Some natural shapes at frequencies higher than 7 kHz are mixed without possibility of comparing to each other. [10][11]

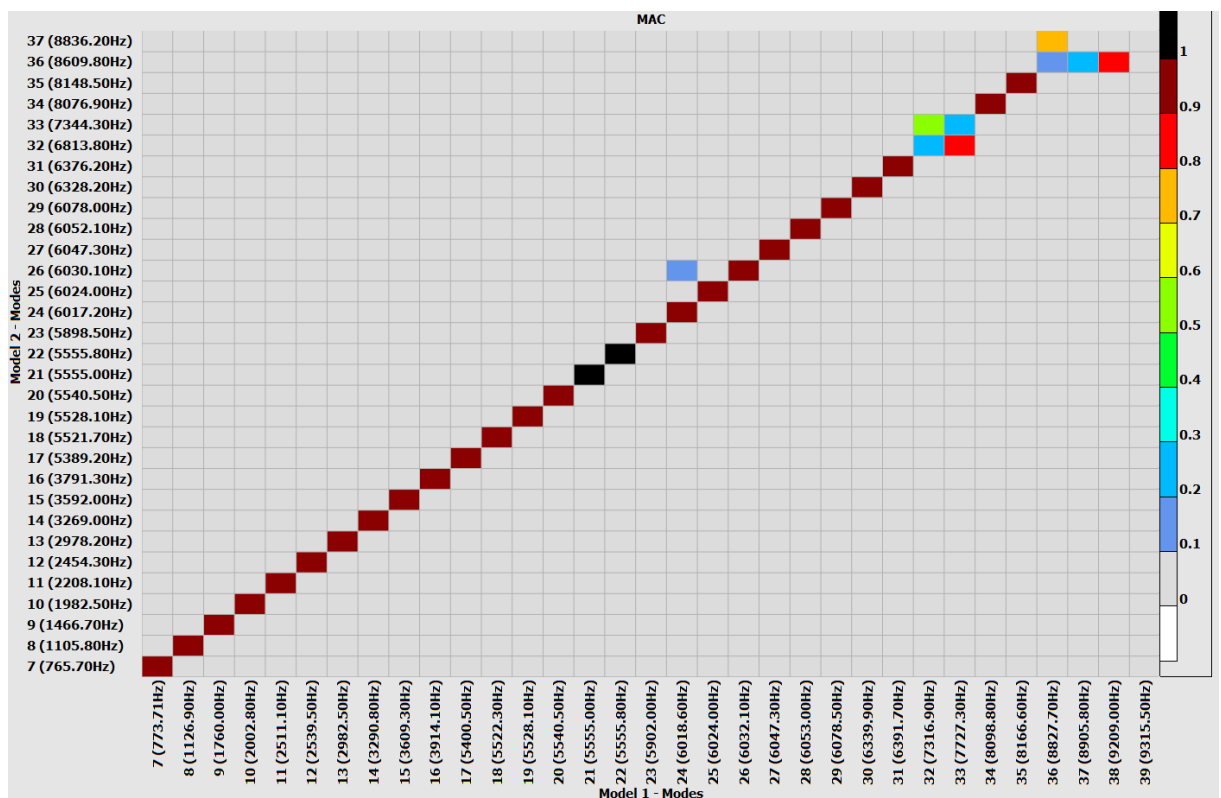


Figure 58 MAC matrix for G_{xz} and G_{yz} change 50%

Important is also range of wires resonance, which consists of 11 eigenfrequencies (modes 18-29). This range moves in dependence on pressure and takes approximately 600 Hz for smaller pad assembly and 900 Hz for bigger pad assembly. This range moves with preloading pressure intensively and can absorb some important eigenfrequencies.

6.2.3 Modal shapes, sensitivity with bigger pad

Some of modal shapes are similar to smaller pad assembly and bigger pad assembly. Because of the different stiffness and mass, they occur at different frequencies. Analogic table 14 and modal shapes (figures 59-64) are shown below.

Table 14 Sensitive modes, bigger pad

Mode	Frequency [Hz]	Sensitive to parameter	Δf [Hz]
7	865	Ez	65
8	2758	Ez	143
9	2968	Gxz, Gyz	271
12	3519	Gxz, Gyz	417
15	4040	Gxz, Gyz	250
33	7370	Ez	303

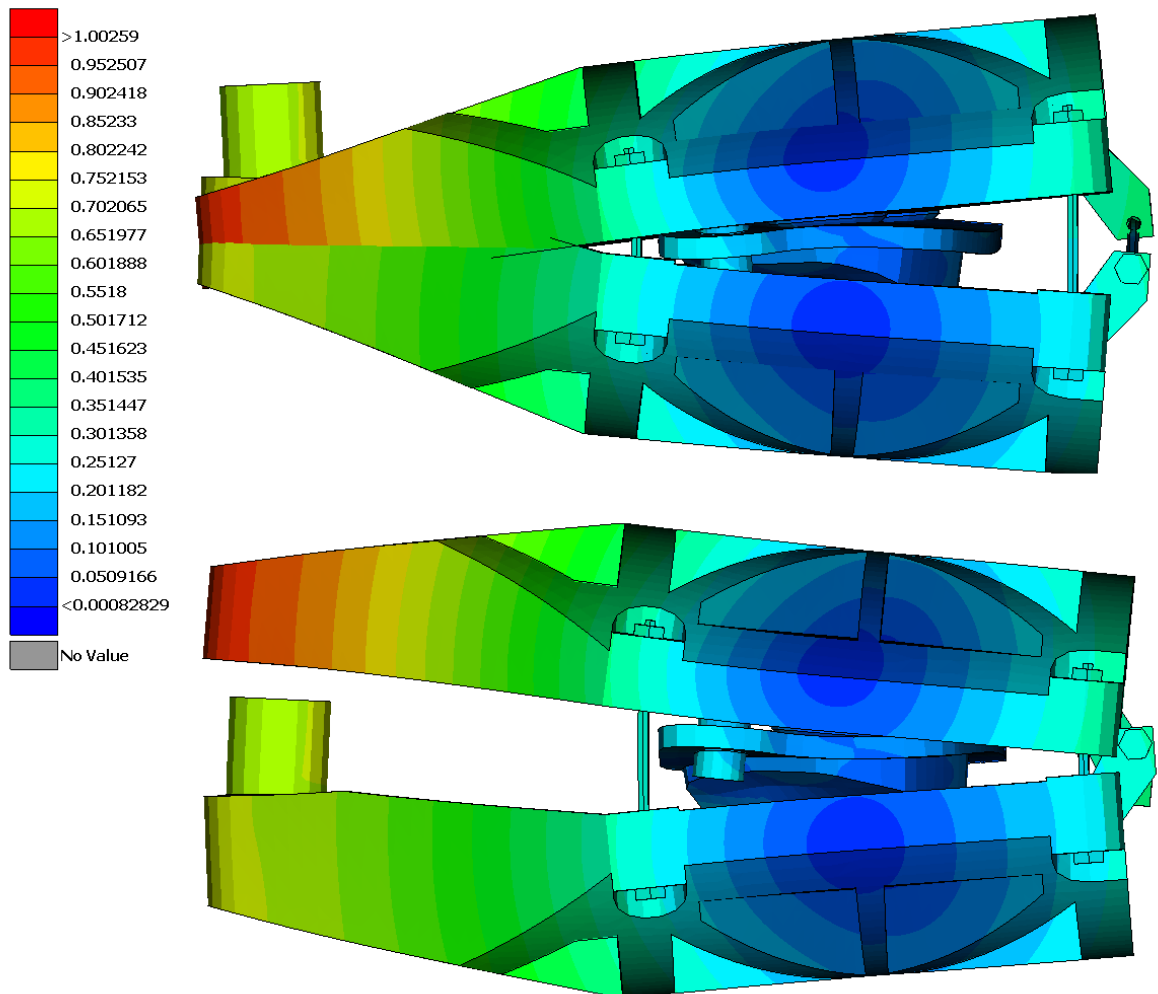


Figure 59 Bigger pad, 7th shape

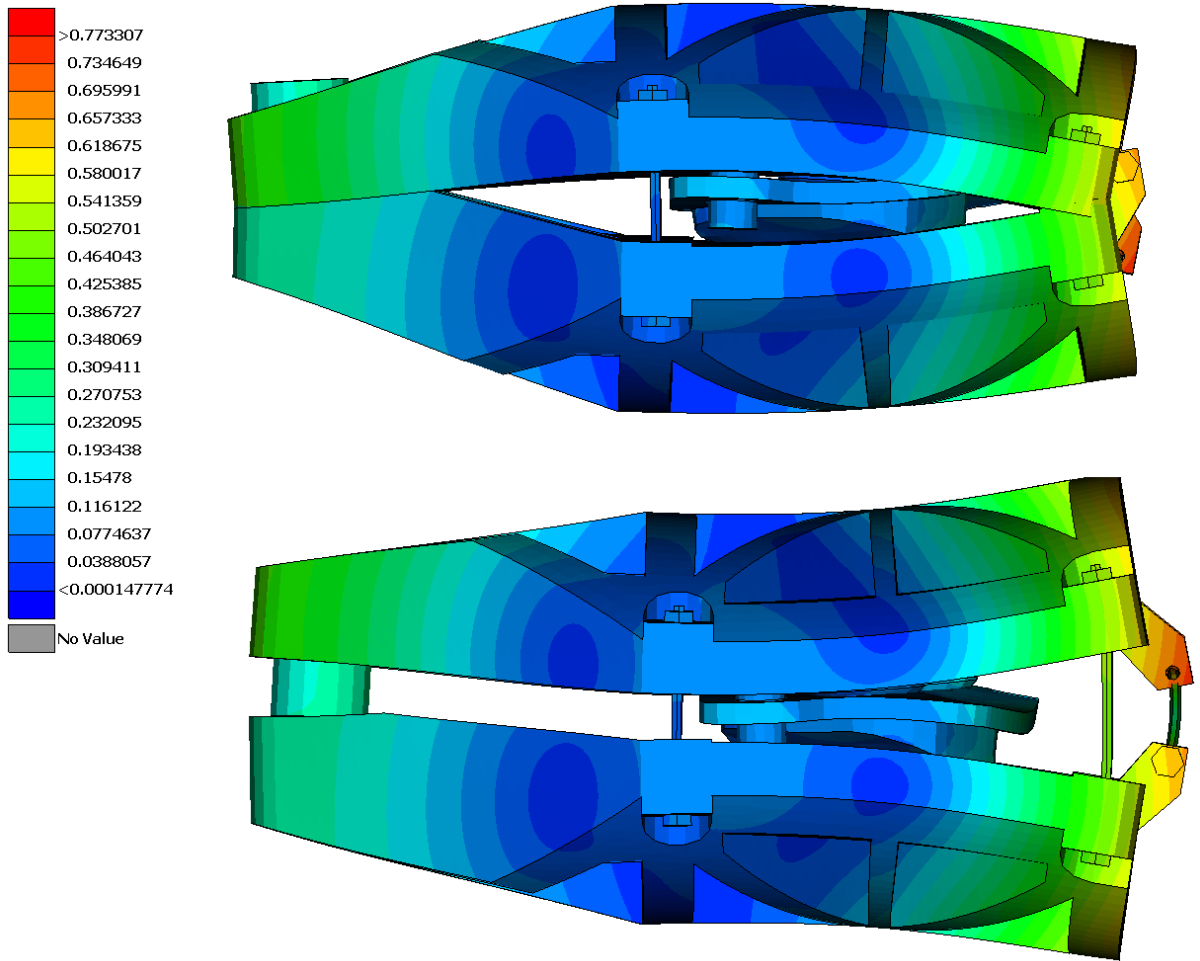


Figure 60 Bigger pad, 8th mode

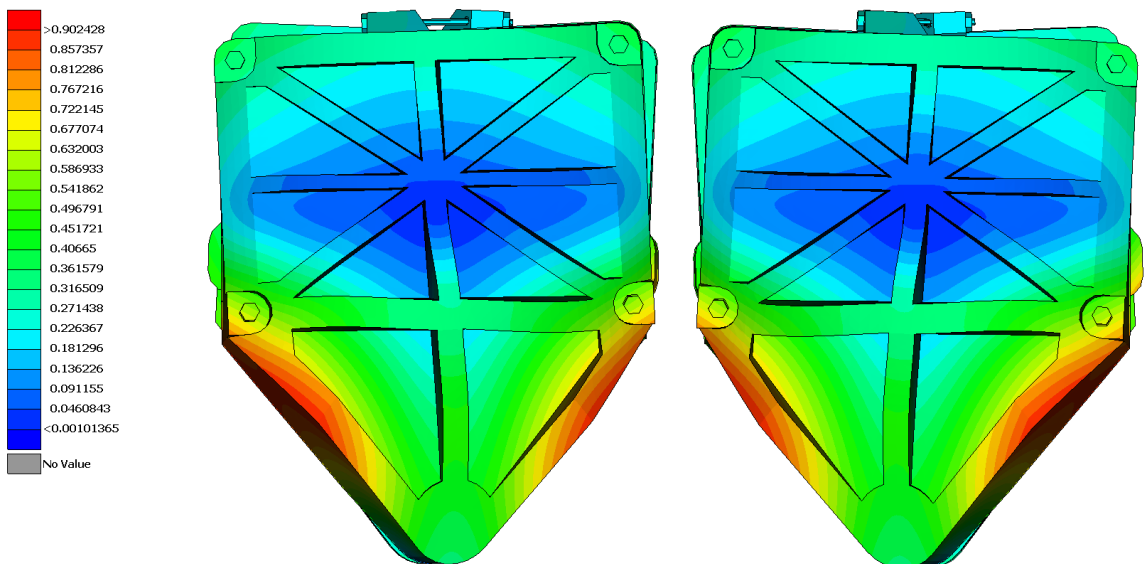


Figure 61 Bigger pad, 9th mode

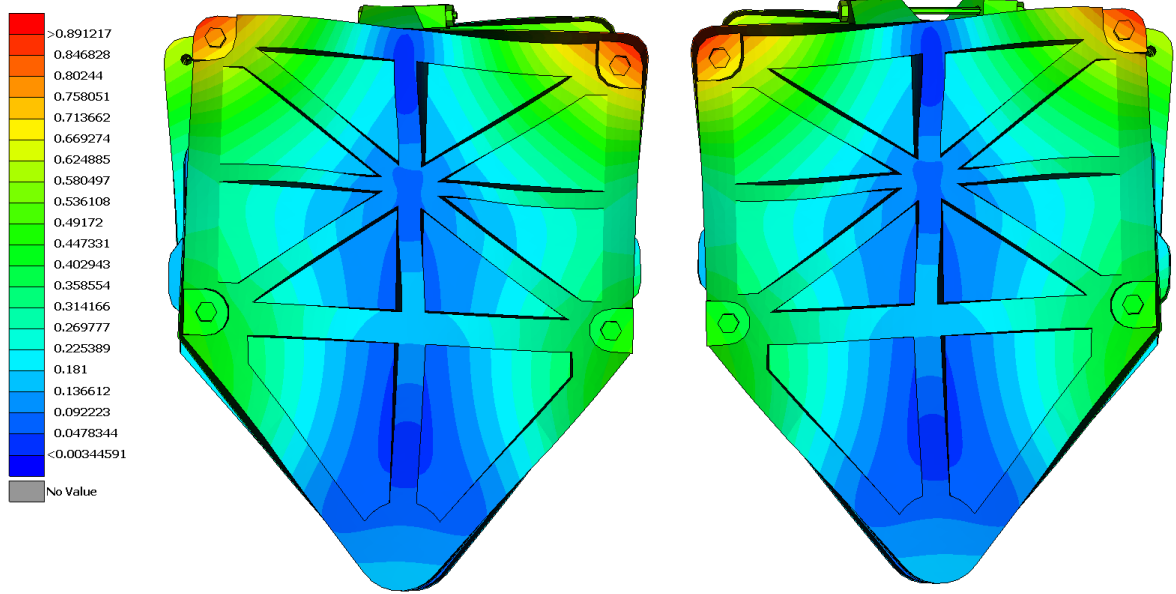


Figure 62 Bigger pad, 12th mode – shear mode

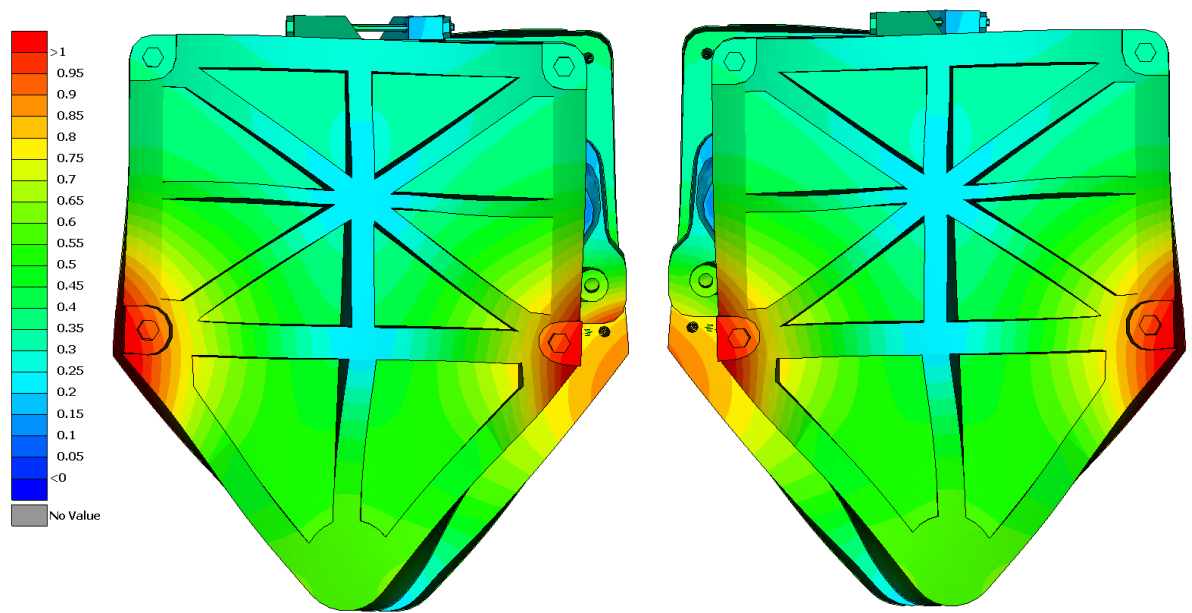


Figure 63 Bigger pad, 15th mode

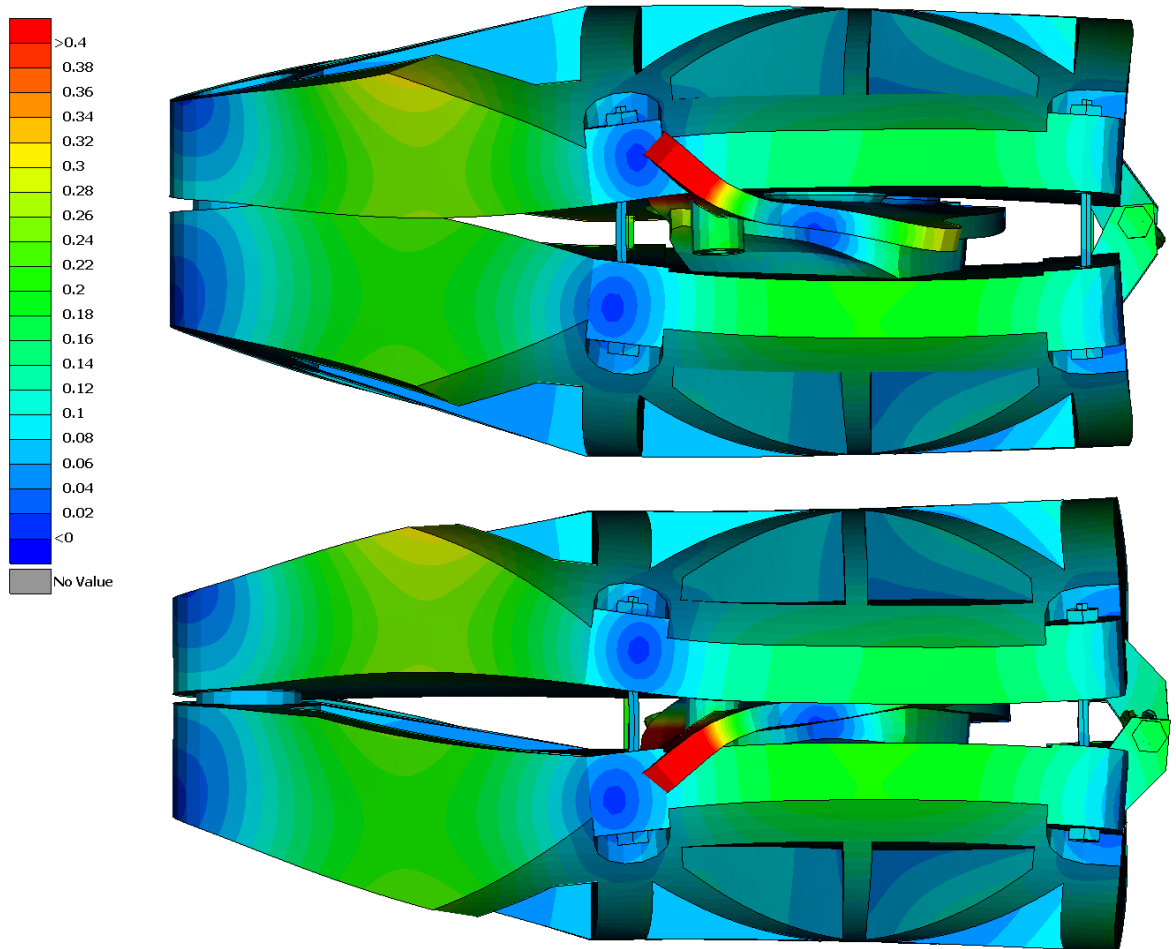


Figure 64 Bigger pad, 33th mode

Bigger pad has significantly larger influence to the whole test behaviour. Although the MAC matrix comparing original material with changed axial Young's modulus (E_z , figure 65) looks similar to analogic one for smaller pad assembly, changing of shear modulus G_{xz} and G_{yz} makes huge difference in shapes. Between 3 kHz and 4 kHz, modal shapes are too different to comparison between them (figure 66). On the other hand, this is the maximal parameter change 50%. When the change is lower, shapes are much more similar and suitable for comparison.

As same as smaller pad assembly, it starts to be sensitive to E_x and E_y parameters at high frequencies (more than 7 kHz). These modes are also sensitive to other material parameters, so description of friction material is not easy.

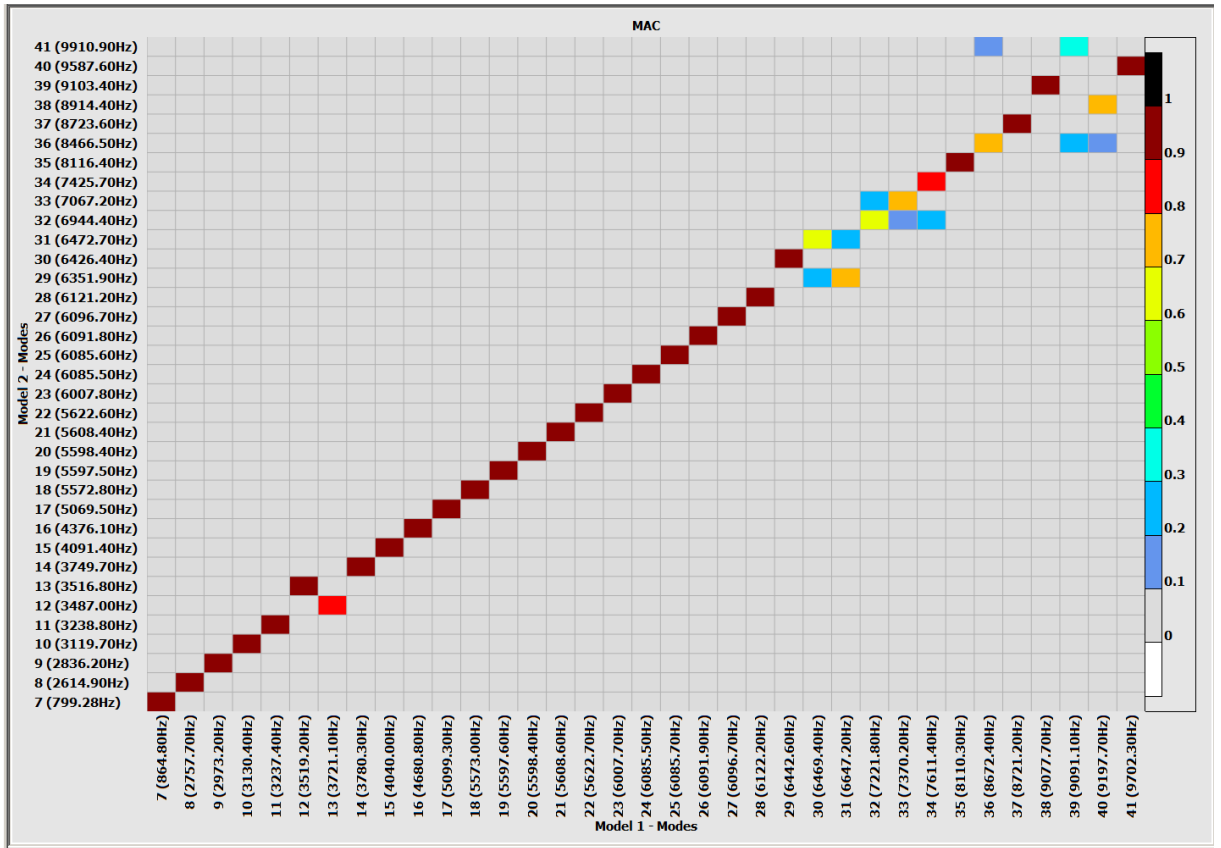


Figure 65 MAC matrix for E_z change 50%

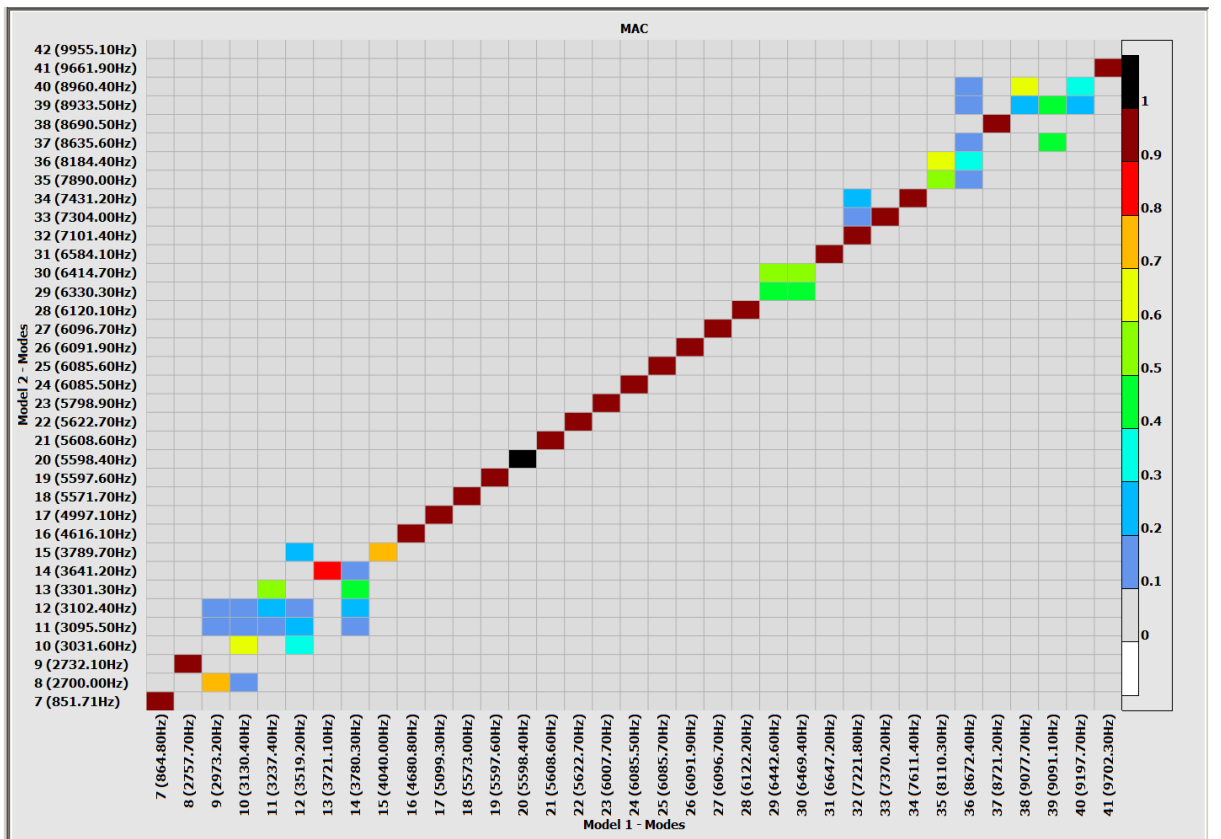


Figure 66 MAC matrix for G_{xz} and G_{yz} change 50%

6.3 Results validity

All the results have to be discussed to verify their validity.

6.2.3 Dependence of eigenfrequency on friction coefficient

For better understanding of tangential preloading, additional analyses of effective friction coefficient were done. Contacts between friction surfaces and the rig were set to ability of transfer the same magnitude of tangential force as a normal force ($\mu=1$). Axial force stayed constant corresponding to 1 MPa and tangential force was increased in several steps. Evolution of real tangential force on the contact surface is shown in figure 67. Next to each picture, preloading force on tangential wire is written. Even though the tangential force on the wire is horizontal, the reaction is directed downward with different magnitude.

Tangential force was measured for computing effective friction coefficient. The goal was to find out dependence of eigenfrequency on effective friction coefficient, which is set by equation:

$$\mu_{ef} = \frac{\Sigma F_t}{F_n}$$

Where the F_t stands for measured tangential force and F_n stands for normal force (also axial force).

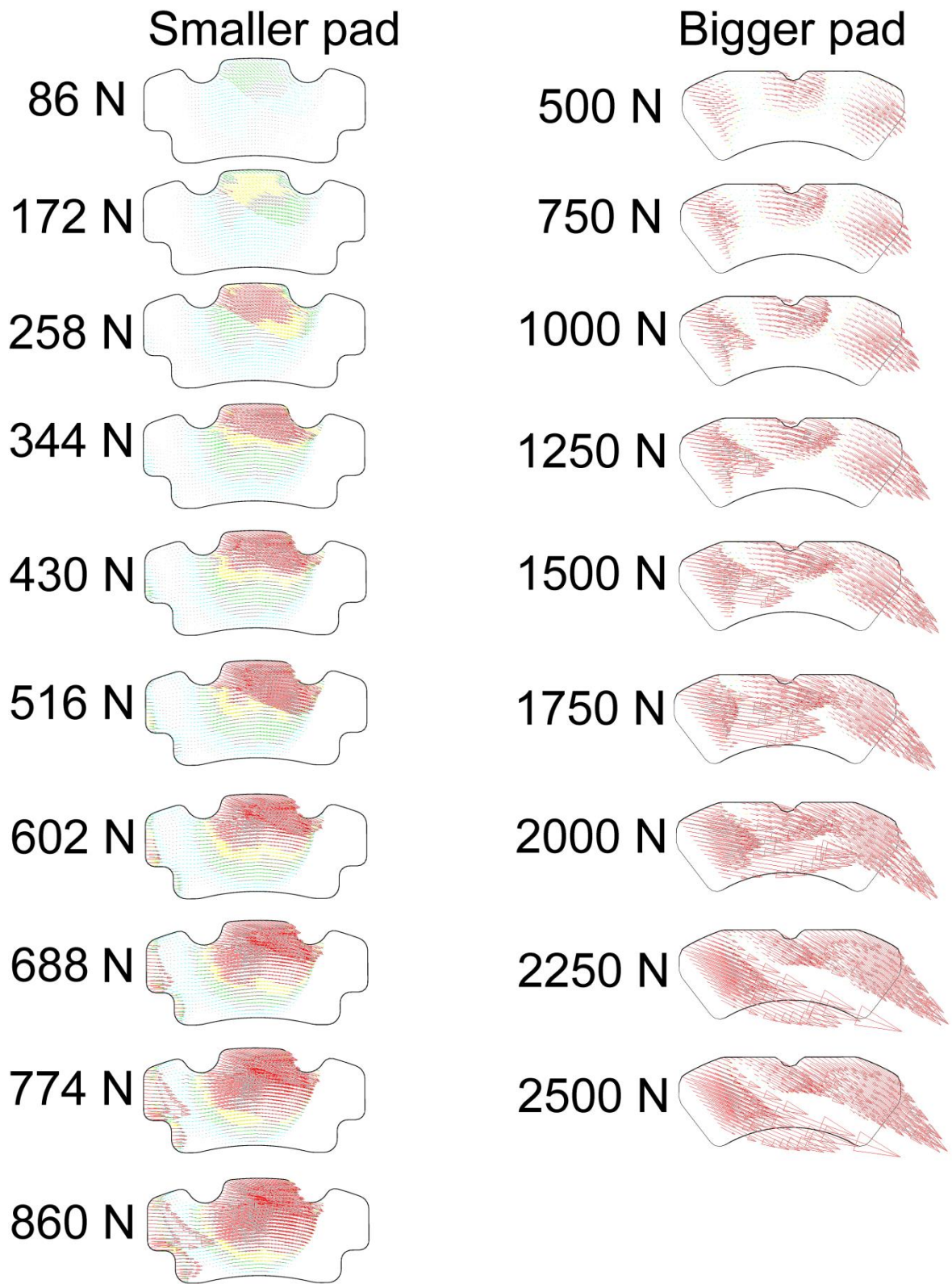


Figure 67 Tangential force evolution

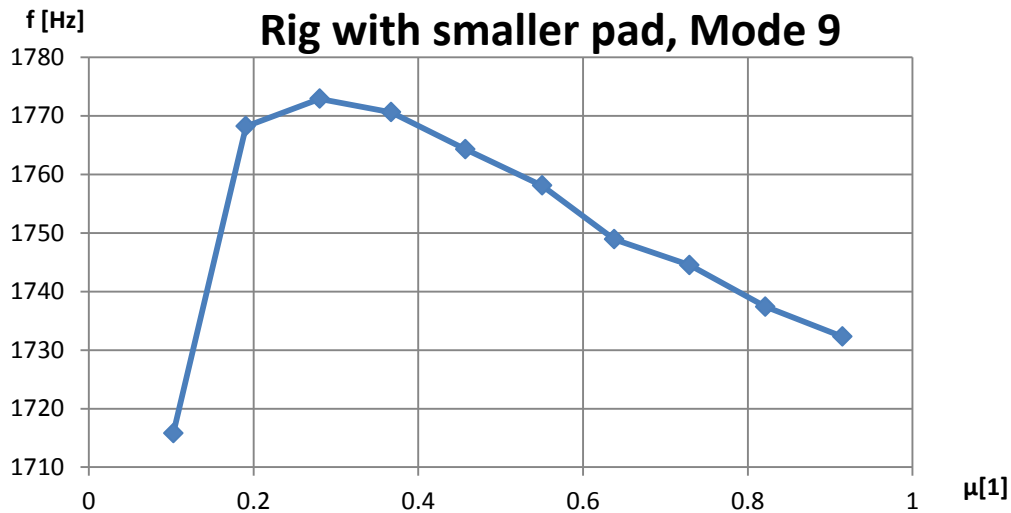


Figure 68 Frequency as a function of friction coefficient, smaller pad

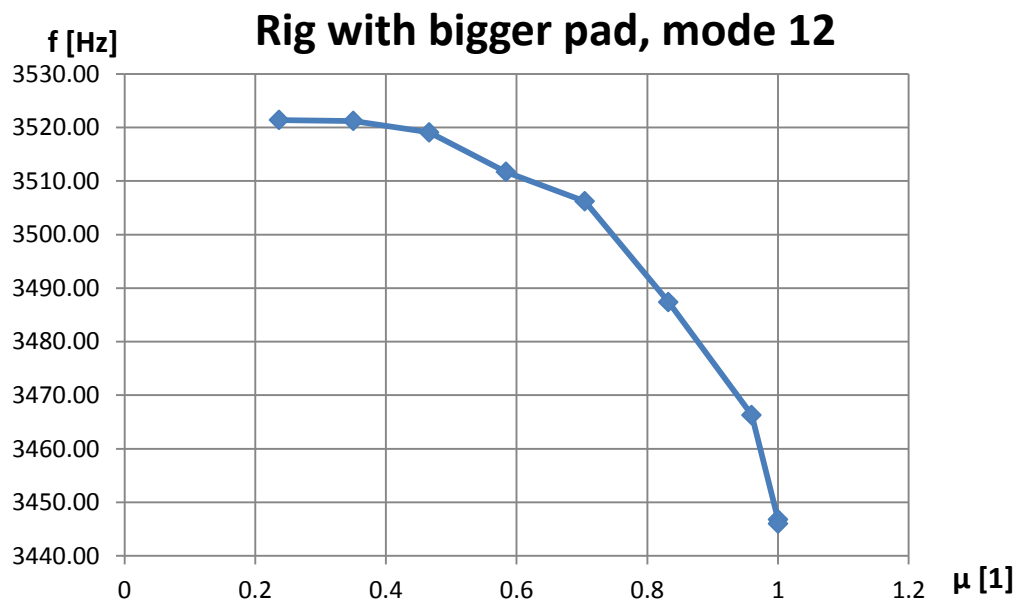


Figure 69 Frequency as a function of friction coefficient, bigger pad

As shown in figures 68 and 69 (shear modes), eigenfrequencies decrease with increasing effective friction coefficient. It is result of contact status changes, because pad slips more with increasing tangential force. In dynamic analyses, its connection area decreases and the whole rig is more compliant.

6.3.2 Bending of the rig

Despite all efforts to reinforce the rig against deformation, preloaded rig is always little bit bent around axis y . It is noticeable in figure 70, where the pressure at middle piston is lower than the pressure at side pistons.

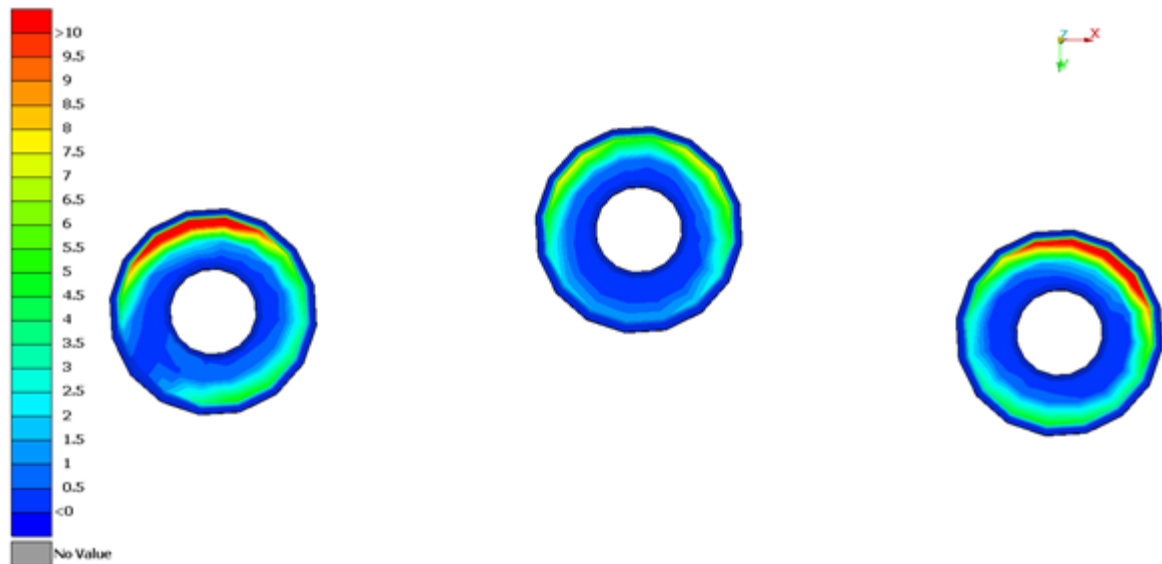


Figure 70 Pressure distribution on pistons, bigger pad

Possible solution is to reinforce area around middle piston, or to make areas around side pistons more compliant. Another way how to avoid different pressure magnitudes is to have middle piston higher than the side ones. On the other hand, pressure distribution on friction surface is not much different to pressure distribution in real caliper, so intervention to the design is not necessary.

7 Conclusions

The test rig provides relatively similar clamping as real brake calipers. Rig pressure distribution and caliper one are much alike. Friction material 50% changes can cause eigenfrequencies changes higher than 10%. It is enough for friction material description from modal analysis results.

On the other hand, damping of the whole model is neglected. Especially the pin constraint can generate significant damping, because there is relative motion in all modal shapes except wires resonance. (4)

For reliable recognizing of friction material, properties of the rig must be accurately known. For true assessment if the rig works correctly, it must be produced and measured. In the CAD model and FE model, there weren't technological radiuses for example between the ribs and around the pistons.

In spite of free modal analysis, the whole rig is sensitive to axial Young's modulus and shear modulus. On the other hand, sensitivity to other material parameters in other directions is limited.

References

1. Renault A, Massa F, Lallemand B, Tison T. Experimental investigations for uncertainty quantification in brake squeal analysis. *J Sound Vib* [Internet]. 2015;367:37–55. Available from: <http://dx.doi.org/10.1016/j.jsv.2015.12.049>
2. Bin Z, Ripin M. Analysis Of Disc Brake Squeal Using The Finite Element Method. 1995;(September).
3. Bakar ARA, Ouyang H, Siegel JE. Brake Pad Surface Topography Part II: Squeal Generation and Prevention. *Sae Tech Pap*. 2005;
4. Olesen HP, Randall RB. A Guide to Mechanical Impedance and Structural Response Techniques (17-179). *Bruel Kjaer Appl Note* [Internet]. 1977; Available from: <http://www.bksv.com/doc/17-179.pdf>
5. Wiertlewski M, Hayward V. Transducer for mechanical impedance testing over a wide frequency range. 2011;
6. Liu P, Zheng H, Cai C, Wang YY, Lu C, Ang KH, et al. Analysis of disc brake squeal using the complex eigenvalue method. *Appl Acoust*. 2007;68(6):603–15.
7. Kung S, Dunlap KB, Ballinger RS. SAE TECHNICAL Complex Eigenvalue Analysis for Reducing Low Frequency Brake Squeal. *Engineering*. 2000;(724).
8. Rahim AbuBakar A, Ouyang H, AbuBakar A, Ouyang H. Complex eigenvalue analysis and dynamic transient analysis in predicting disc brake squeal. *Int J Veh Noise Vib J Veh Noise Vib*. 2006;2(2):143–55.
9. Bilošová A. Modální zkoušky [Internet]. first. Ostrava: Skripta VŠB - TU Ostrava; 2012. 129 p. Available from: <http://projekty.fs.vsb.cz/147/ucebniopory/978-80-248-2758-2.pdf>
10. Vacher P. Extensions of the MAC criterion to complex modes. *Proc ISMA ...* [Internet]. 2010;2713–26. Available from: http://www-04.mech.kuleuven.be/past/conf/isma2010/proceedings/papers/isma2010_0103.pdf
11. Pastor M, Binda M, Harčarik T. Modal assurance criterion. *Procedia Eng*. 2012;48:543–8.
12. Semiconductor F. Accelerometer Terminology Guide. *Sensors* (Peterborough, NH). 2007;

13. AUTOMATIZACE.HW.CZ, Principy akcelerometrů [Online] Available from: <http://automatizace.hw.cz/clanek/2007011401>
14. HBM.COM, CFW Piezoelectric washer [Online] Available from: <https://www.hbm.com//en/2919/paceline-cfw-measuring-piezoelectric-force-washer/>
15. NOSHOK.COM, 3540 Series Tension & Compression Force Transducers [Online] Available from: http://www.noshok.com/force_3540_series.shtml
16. MOODLE.FS.CVUT.CZ, Electromagnetic Actuators [Online] Available from: <https://moodle.fs.cvut.cz/pluginfile.php/7448/course/section/1818/Electromagnetic%20actuators.pdf>